

Electron Probe Microanalysis

RAYMOND CASTAING

Département de Physique Générale, Faculté des Sciences, Université de Paris, Orsay, France

	<i>Page</i>
I. Introduction.....	317
A. Old Methods of Quantitative Determination.....	318
B. An "Absolute" Method Using Pure Elements as Standards.....	319
C. Emission-Concentration Proportionality Law.....	320
II. General Structure of the Microanalyzer.....	324
A. The Electron Probe.....	326
B. Thermal Conditions of the Analysis.....	337
C. Contamination.....	339
D. X-ray Recording.....	340
E. Localization of the Analysis.....	347
III. The Fundamentals of Quantitative Analysis by X-Ray Emission.....	360
A. Absorption Correction.....	361
B. Distribution in Depth of the Characteristic Emission.....	362
C. The Physical Basis of the Emission-Concentration Relation.....	366
D. Experimental Absorption Correction Curves.....	370
E. Fluorescence Correction.....	371
F. Fixed-Time versus Fixed-Charge Measurements.....	376
IV. The Contribution of Microanalysis to Scientific Research.....	379
A. Metallurgy.....	380
B. Mineralogy.....	383
C. Technical Studies.....	384
References.....	384

I. INTRODUCTION

The spot analysis technique known as "electron probe microanalysis" or "X-ray microanalysis" was developed ten years ago by the author in his thesis prepared under the direction of Prof. A. Guinier (1-3). The principle of the method is as follows: a finely focused electron beam (electron probe), of a diameter less than $1\text{ }\mu$, is directed onto a particular point of the surface of a sample whose chemical composition is to be examined. The very small volume of material irradiated by the electron beam (about one cubic micron) then emits a complex X-ray spectrum which includes the characteristic radiations of the various elements present at the point of impact of the probe. Spectrographic analysis of this X-ray spectrum permits the respective concentrations of these elements to be determined.

Such a principle was hardly novel: it can be observed that the apparatus (Fig. 1) used by Moseley (4) in his historical work on the frequencies of

characteristic X lines contains, with its trolley carrying various targets under an impinging electron beam, all the main elements of an electron probe microanalyzer. Ten years after the epoch-making experiments of Moseley, the first applications of X-ray spectrography to chemical analysis were beginning to bear fruit; these mainly concerned the analysis of powders. In this field, X-ray emission had from the very first some remarkable successes, in particular, the discovery of new elements. In this connection

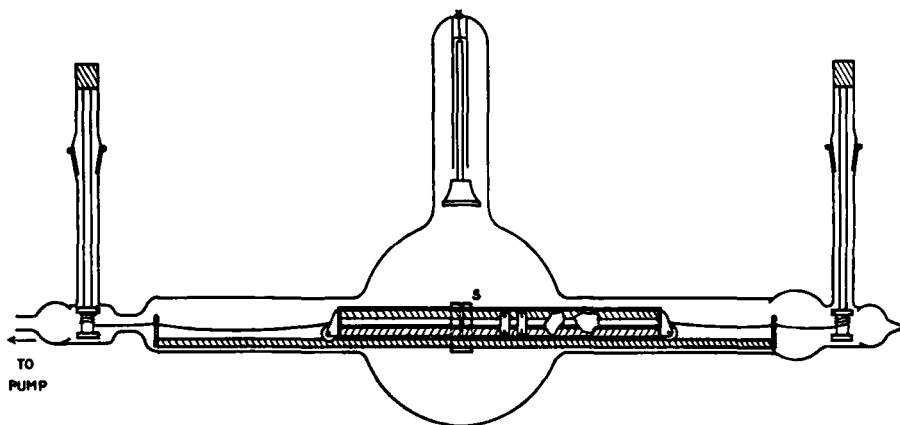


FIG. 1. Moseley's apparatus (by courtesy of Philosophical Magazine).

one may mention the discovery of element 72, whose $L\alpha_1$ and $L\beta_2$ lines were first identified by Urbain and Dauvillier (5) and whose entire L spectrum was obtained a little later by Coster and von Hevesy (6).

The extreme simplicity of X-ray spectra where, contrary to the case of light spectra, the characteristic lines are few and practically insensitive to chemical bonds, led physicists to consider the problem of quantitative analysis. The wavelengths of the various characteristic radiations made it possible to define the nature of the elements present in the sample. There remained to deduce from the intensities of these various radiations the relative proportions of the constituent elements; and then many difficulties began to appear. These difficulties will be reviewed briefly; it will be shown that the main advance brought about by the electron probe microanalyzer results more from the principle involved in quantitative analysis than from the spot character of this analysis.

A. Old Methods of Quantitative Determination.

For many years, quantitative analysis by means of X-ray spectrography proceeded on the essentially empirical method used by the early workers.

The principle was as follows: Let us suppose we have to determine the concentration of an element A in a mixture (generally a mixture of oxides in powder form). The mixture is deposited on the anticathode of an X-ray tube and is subjected to bombardment by the beam. A measurement is made (generally by simple photographic recording of the spectrum) of the intensity with which the mixture emits, under definite bombardment conditions, the most important characteristic line of the element A. There is then added to the mixture increasing quantities of a reference element B, with an atomic number close to that of element A, until the homologous characteristic lines of elements A and B are emitted with the same intensity by the mixture. It is then taken that the concentration of element A is equal to that of the reference element B.

This method of determination has the double disadvantage of being highly complex and rather inaccurate. Even when precautions are taken to avoid selective volatilization of one of the constituents under the impact of the electron beam, many other sources of error make the results very uncertain. For example, the method is based on the comparison of the intensities of two radiations of different wavelength. These two radiations are adsorbed differently in the sample, in the output window of the tube, and in air; they are reflected with a different efficiency by the crystal and recorded with different sensitivity by the receiver unit of the spectrometer; so the ratio of the measured intensities differs appreciably from the ratio of the intensities actually emitted by the sample. It becomes necessary to apply rather uncertain corrections, which depend essentially on the experimental arrangement. If an attempt is made to reduce these causes of error by choosing lines of extremely close wavelengths, one is led to comparing lines of different kinds (for example, the $L\alpha_1$ line of element A and the $L\beta_1$ line of element B) and the ratio of line intensities for equal concentrations has to be empirically estimated. And moreover, the X-ray lines of two distinct elements, even of very close wavelengths, generally have distinctly different excitation thresholds, with regard to both direct excitation by the electron beam and secondary fluorescence excitation.

Under such conditions it is necessary for the determination to proceed in an empirical manner, calibration from mixtures of known composition being essential in practice.

B. An "Absolute" Method Using Pure Elements as Standards

It has just been stated that the main source of inaccuracy in old methods of X-ray spectrographic analysis rests on the fact that they are based on the comparison of the intensities of two radiations of different wavelengths or kinds. For this reason, the author (2) has proposed a method of analysis based on a new principle in which comparisons of intensity are made on

identical radiations. Measurements thus have an intrinsic significance and are not affected by properties characteristic of the apparatus used.

In this new method, the concentration of an element A in a given alloy is deduced from a comparison between the intensity I_A of an important characteristic line of element A emitted by the alloy under given conditions of electron bombardment and the intensity $I(A)$ of the same characteristic radiation when emitted by the pure element A under the same electron bombardment conditions.

The operation consists of taking two readings on the spectrometer, by successively bringing under the impact of the electron beam the region of the sample to be analyzed and an element for comparison in the form of the pure element A. The main advantage of this method lies in the fact that the simple ratio of two readings supplies with good accuracy the mass concentration of element A in the region analyzed, as was shown by the author (2) and later by Castaing and Descamps (7) in a more rigorous treatment.

C. Emission-Concentration Proportionality Law

It is assumed that the sample, homogeneous over an extensive region, contains n elements A_i of respective mass concentrations c_i ; it is desired to determine the mass concentration c_A of one of these constituents, such as A. For this purpose, the emission I_A of the sample in the $K\alpha_1$ line of element A is compared with the emission $I(A)$, in the same line A $K\alpha_1$ and under the same electron bombardment conditions, of a reference target consisting of the pure element A. Let us show that the concentration of element A in the region analyzed is supplied, as a first approximation, by the simple relation $I_A/I(A) = c_A$.

Consider the trajectory of an electron within the sample. Along this trajectory, the energy E of the electron passes from $E_0 = eV$ (V being the accelerating voltage of the beam) to zero, this energy E being a function of the path x followed from the point of impact. Let $E_K = eV_K$ be the critical excitation energy of the K level of element A, and n_K the number of electrons $K(A)$ present per cubic centimeter in the sample. The number of $K(A)$ ionizations produced along the path dx is then $dn = \Phi(E, E_K, n_K)dx$; the ionization function Φ contains n_K as a factor, and designating ρ as the density of the analyzed region, A the atomic weight of element A, and ψ_A a function depending only on the characteristics of element A, we can write

$$dn = \frac{\rho c_A}{A} \frac{\psi_A(E) dE}{dE/dx}. \quad (1)$$

As a first approximation let us assume that Williams' law (8) applies to the deceleration of the electron

$$\frac{dE}{dx} = k\rho\beta^{-1.4} \quad (2)$$

where k is a constant and $\beta = v/c$ is a function only of the energy E of the electron; we have

$$dn = \frac{c_A}{A} f_A(E) dE, \quad (3)$$

the function f_A depending only on the characteristics of element A. The total number of $K(A)$ ionizations produced by the electron along its trajectory is then

$$n = \frac{c_A}{A} \int_{E_0}^{E_K} f_A(E) dE. \quad (4)$$

The same electron would have produced in the pure element A a number of ionizations

$$n' = \frac{1}{A} \int_{E_0}^{E_K} f_A(E) dE.$$

We have assumed that the characteristics of the electron beam and the adjustment of the spectrometer remain the same for the two successive measurements.

Neglecting for the present the X-ray absorption in the sample itself and the secondary fluorescence emission, points which will be taken up again later, it is clear that the ratio $I_A/I(A)$ of the intensities seen on the spectrometer is equal to the ratio n/n' of the number of ionizations produced by an electron in the region analyzed and in the pure element A. From this the required relation is derived which is valid as a first approximation

$$\frac{I_A}{I(A)} = c_A. \quad (5)$$

In a second approximation we can take for the deceleration of the electrons the law proposed by Webster (9) which, for a pure element A of atomic number Z_A , is

$$\frac{dE}{dx} = k\beta^{-1.4}\rho_A 2 \frac{Z_A}{A}, \quad (6)$$

and which becomes, for the complex anticathode,

$$\frac{dE}{dx} = k\beta^{-1.4} 2\rho \sum \frac{c_i Z_i}{A_i}. \quad (7)$$

The same calculation then leads to the relation

$$\frac{I_A}{I(A)} = \frac{c_A Z_A / A}{\sum c_i Z_i / A_i}. \quad (8)$$

If we designate by n_i the number of atoms A_i per unit volume in the sample, the two approximations considered may be written

$$\frac{I_A}{I(A)} = \frac{n_A A}{\sum n_i A_i}, \quad \frac{I_A}{I(A)} = \frac{n_A Z_A}{\sum n_i Z_i}.$$

It is clear that the validity of these approximations is not tied to the exact form of the deceleration laws of Williams or Webster, since, in order for the first approximation to be valid, it is only necessary that the deceleration law of the electron along its path be written $dE/dx = \rho\varphi(E)$, whereas the second approximation assumes that the deceleration law can be written $dE/dx = n\psi(E)$, n being the number of electrons per unit volume of the sample and the functions φ and ψ being any functions of the argument E .

Neither of these two deceleration laws, of course, is rigorously obeyed and a still better approximation could be obtained by applying to each of the elements A_i a coefficient α_i representing its "specific deceleration power," so that the deceleration law of the electron in the pure element A_i of specific weight ρ_i may be written $dE/dx = \alpha_i \rho_i f(E)$, where f is a universal function of any form. The emission-concentration relation would then take the form

$$\frac{I_A}{I(A)} = \frac{\alpha_A c_A}{\sum \alpha_i c_i}. \quad (9)$$

It is the latter form which would have to be adopted as a second approximation, the coefficients α_i being empirically adjusted by means of measurements made on alloys of known composition. The validity of this last approximation holds only on the assumption that the deceleration curves of the electrons in the various elements can be deduced from each other by expansion or contraction of the coordinates.

It should now be noted that, in order to simplify the calculations, we made two assumptions the validity of which requires examination.

(1) We have neglected the X-ray absorption in the sample itself and the secondary fluorescence emission; in fact, such a simplification is generally not admissible. Actually, the foregoing relations are valid only for the intensities emitted *in the sample* (i.e. corrected for their absorption in the sample itself) *from atoms directly ionized by the electrons of the beam*. It will therefore be necessary, after each measurement, to deduct from the measured intensity the fraction of this intensity corresponding to a secondary fluorescence emission. It will be seen later that these various corrections can be sufficiently well estimated so they do not affect the accuracy of the measurement.

(2) It has been implicitly assumed that the trajectory of the electron,

or at least that part of the trajectory where the electron has an energy greater than the critical excitation energy of the X-ray level, is entirely within the sample. This assumption is incorrect because of back-scattering. We shall see further that back-scattering tends to raise the apparent concentration of the heavy elements and so acts in the opposite direction to the factor Z/A of the Webster equation [Eq. (6)]. This effect produces a kind of compensation with the result that the validity of the first approximation, which assumes strict proportionality between emission and concentration, is often much better than might have been supposed.

In any case, back-scattering can be taken into account by a suitable choice of the empirical coefficients α_i , and the following basic relations can be written between the intensities and the concentrations

$$\frac{I_A}{I(A)} = c_A, \quad (\text{first approximation}) \quad (10)$$

$$\frac{I_A}{I(A)} = \frac{\alpha_A c_A}{\sum \alpha_i c_i}. \quad (\text{second approximation}) \quad (11)$$

It is understood that these relations are with respect to the intensities corrected for their absorption in the anticathode and for the fraction due to a secondary fluorescence excitation. We shall return later to the validity of these relations, which has been verified experimentally for a considerable number of analyses carried out on homogeneous samples of known composition.

Stress should be laid on the fact that the reason for the simplicity of the relations rests mainly on the absolute character of the measurements: the radiations whose intensities are being compared have the same wavelength, and all the difficulties which might arise from the absorption of the radiation—apart from that in the sample itself—or from the efficiency of the spectrometer are automatically eliminated since they occur equally for both terms of the ratio. The quotient of the two readings (after correction for fluorescence and self-absorption) very accurately gives the ratio of the over-all emissions, in the line analyzed, of the sample and of the pure element; this ratio has an intrinsic significance which is independent of the experimental equipment.

The absolute character of this method of analysis makes superfluous the use of reference samples with a composition close to that of the sample to be examined, whereas such practice is essential in light spectrography, for instance. This circumstance is a particularly happy one, and the method would hardly be usable as a quantitative analytical method did it not possess this absolute character. It would be impossible to prepare a whole series of reference samples with sufficient small-scale homogeneity. In the

field of metallurgy, for instance, definite phases or solid solutions (which, however, may contain submicroscopic precipitates) alone are usable as standards for local analysis. Even in the case of binary alloys, definite phases, if such there be, are few in number; the concentration of solid solutions can be varied continuously, but over a range which is generally narrow in the neighborhood of pure elements. Last, it is generally impossible to obtain phases containing more than two elements and of sufficiently well-known composition to be used as standards; in fact, the precise role of electron probe microanalysis will be to determine the composition of these multiple phases which generally appear as small precipitates.

II. GENERAL STRUCTURE OF THE MICROANALYZER

The principal elements of a conventional electron probe microanalyzer are four in number:

(1) An electron optics system, consisting of an electron gun followed by reducing lenses, whose role is to produce at the level of the sample an electron probe with a diameter approximately between the limits of 0.1 and 2 μ . It will be seen that, in the present state of technique, diffuse penetra-

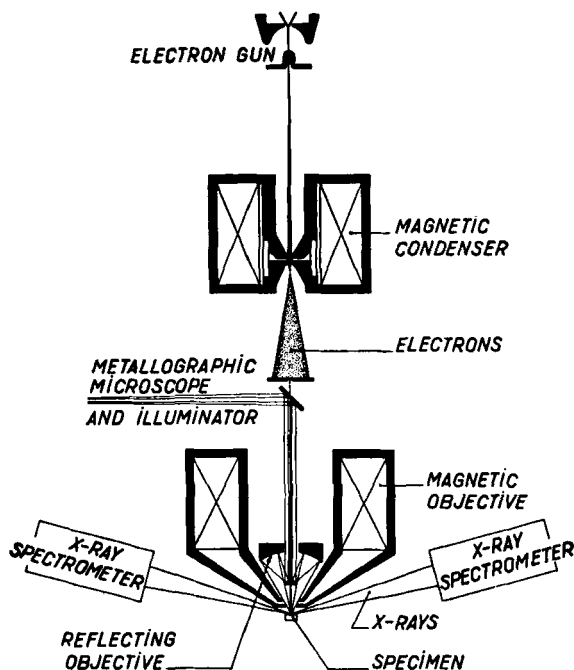


FIG. 2. Schematic diagram of the French microanalyzer (Castaing and Descamps).

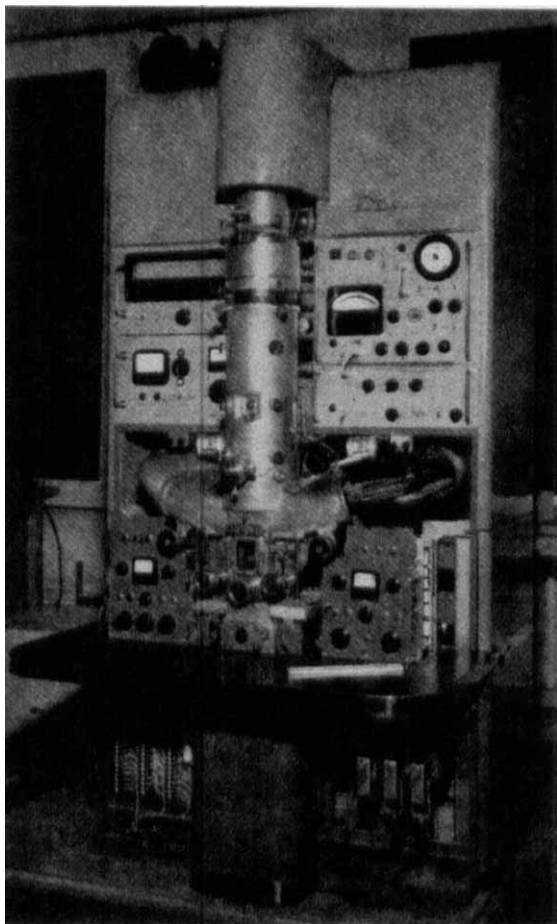


FIG. 3. The French microanalyzer (Castaing and Descamps). Parts of the housing have been removed and the right-hand spectrometer has been opened to give an inside view.

tion of electrons in matter makes it unnecessary, at least for the analysis of massive samples, to use probes of very small diameter.

(2) A mechanical arrangement for bringing successively under the probe the point of the sample to be analyzed and the reference targets consisting of the pure elements or of compounds of known composition.

(3) A viewing device (generally a metallographic microscope) for accurately choosing the point to be analyzed.

(4) A set of spectrometers for analyzing the X-ray radiation emitted.

The first experimental model built by the author in 1949 by converting

a C.S.F. electron microscope (1-3), used electrostatic reducing lenses and a single spectrometer in air. The latter practically prohibited the analysis of light elements. Since then, many more or less improved models have appeared in various countries. We shall describe here in detail the apparatus built by the author in the laboratories of the Office National d'Etudes et de Recherches Aéronautiques. This instrument, shown at the French Physical Society's Exhibition in June 1955, is now available commercially and it will be referred to here as "the French model." Figure 2 shows diagrammatically the principle of the apparatus, a general view of which is given in Fig. 3.

A. The Electron Probe

The probe is obtained by forming, by means of electron lenses, a much reduced image of the crossover produced by an electron gun. The gun is of the conventional hot cathode triode type; the three models which are most frequently used are shown in Fig. 4. The French model uses a type *A* gun

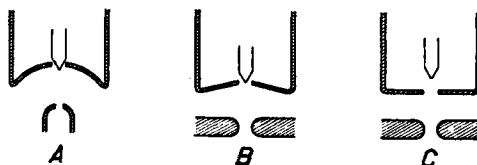


FIG. 4. Three usual models of electron guns.

which was designed by Bricka and Bruck (10) for the C.S.F. electron microscope. This gun concentrates in an electron beam of very small aperture almost the total current of the HT source. Its efficiency is excellent and it has the advantage of producing a crossover located immediately below the anode level, in a region where it is easy to place a fixed aperture. The type *B* gun, used in particular by Mulvey (11), has similar properties. As regards type *C* (RCA gun) used by Birks and Brooks (12) its efficiency is lower but its emission seems to be less sensitive to accidental decentering of the filament (warping may shift the filament position). All these guns use a dropping resistor for self-bias operation; Marton and Simpson (13) on the contrary, use a long-focus gun with fixed battery bias.

In The French model, the tungsten filament is heated at high frequency and the HT, stabilized by a conventional electronic process to a few parts in a hundred thousand, is adjustable from 5 kv to 35 kv; for it is essential that the HT used be adapted to the critical excitation energy of the X-ray line being measured.¹

The electron gun is followed by two magnetic reducing lenses (Fig. 2);

¹ See Sec. II, E, 2.

the first of these lenses has a focal length which is variable between 2 mm and infinity; it acts as a condenser and the adjustment of its excitation makes it possible to obtain probes with a diameter of 0.1 to 3 μ .

The second reducing lens (probe-forming lens) accurately focuses the electron beam on the surface of the sample. Its focal length is about 0.9 cm and its spherical aberration coefficient $C_s = 3.6$ cm. The point of formation

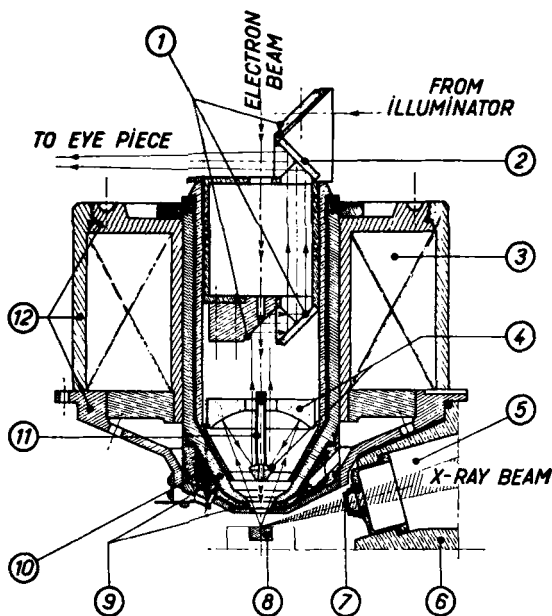


FIG. 5. Probe-forming lens and viewing device (French microanalyzer) (Castaing and Descamps). 1.—Mirrors, 2—semitransparent mirror, 3—coil, 4—reflecting objective, 5—X-ray spectrometer (operating in air, in low vacuum or in high vacuum), 6—main frame, 7—outlet window (can be turned down during work), 8—specimen, 9—pole pieces, 10—stigmator (astigmatism correction and probe deflection), 11—electrostatic shield, 12—lens casing (iron circuit).

of the probe is 0.6 cm below the lower face of the pole piece, which gives sufficient clearance to pass the X-ray beams to be analyzed (Fig. 5). An electrostatic device corrects the natural astigmatism of the probe-forming lens; it also makes it possible to apply to the probe small lateral displacements to compensate for slight deviations which sometimes occur in the analysis of magnetic samples.

Last, on the extension of the beam and about 30 cm below the object level, a fluorescent screen is inserted for observing the beam, which is most useful for certain adjustments; a photographic chamber also provides

means for obtaining electron-diffraction patterns (accurate measurement of the beam accelerating voltage).

Figure 6 shows three types of pole pieces which may be used for the probe-forming lens. Type *A* (French model) accommodates optical viewing of the sample along the beam axis; type *B* (Fisher) is designed for about 1:1 demagnification as a transfer lens; it accommodates lateral viewing of the sample, but its spherical aberration is larger than that of type *A*. With

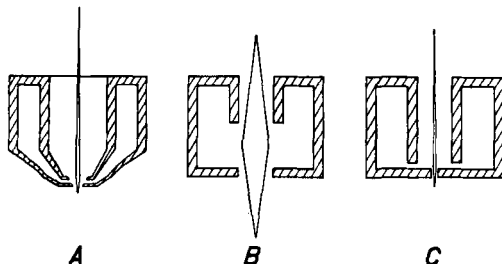


FIG. 6. Three usual models of probe-forming lenses.

the pinhole type *C* (Mulvey) optical viewing of the specimen is impossible, but it has the advantage of reducing the magnetic field strength at the sample level, leading to minimum beam deflection with ferromagnetic specimens.

1. Probe Brightness. Theoretical limitations. The aim is naturally to obtain maximum electron intensity on a probe with the smallest possible diameter, in order that the analysis may add high sensitivity to high resolving power. If electron lenses free of aberrations were available, and more particularly lenses free of spherical aberration, it would be possible to reduce the diameter of the probe by a considerable factor without reducing the current carried by the electron beam, and very high electron densities could be obtained. Unfortunately such is not the case in the present state of technique, and the spherical aberration of the probe-forming lens—the only one working at relatively large aperture—sets a limit to the current that can be obtained in a probe of a given diameter. This limit can be calculated as follows (2):

According to Langmuir (14) the current density in a crossover is a maximum at the center where it is equal to

$$i = i_0 \left(\frac{eV}{kT} + 1 \right) \sin^2 \beta. \quad (12)$$

In this equation, i_0 is the emissive power of the cathode, expressed in amperes per square centimeter; T is the absolute temperature of the

cathode, V is the accelerating potential, and β is the half aperture of the beam at the crossover level.

This amounts to saying that the crossover may be considered as a source of electrons whose brightness (at least at the center) is

$$B = \frac{i_0 e V}{\pi k T}, \quad (13)$$

neglecting unity compared to eV/kT . The successive images of the crossover produced by the various reducing lenses are formed in constant potential media, so that the brightness of the probe is again equal to B . If the reducing lenses were perfect, a probe of Gaussian diameter d_0 formed by a beam with an aperture u would have a true diameter d_0 and would carry an electron current

$$i = \frac{\pi d_0^2}{4} \frac{e V}{k T} i_0 u^2 \quad (14)$$

(u is supposed to be small), and it would only be necessary to increase u in order to increase the current without changing the diameter of the probe. We must, however, take into account the spherical aberration of the probe-forming lens, which spreads the current i over a probe of true diameter $d = d_0 + C_s u^3/2$. This gives, in a probe of true diameter d formed by a beam of aperture u , an electron current

$$i = \frac{\pi}{4} \left(d - \frac{C_s u^3}{2} \right)^2 \frac{e V}{k T} i_0 u^2, \quad (15)$$

where C_s is the coefficient of spherical aberration. This expression has a maximum value for

$$u = \left(\frac{d}{2C_s} \right)^{1/3}, \quad (16)$$

that is, for an aperture such that the diameter of the aberration disk is equal to one-quarter of the true diameter of the probe. The maximum value of the current is then equal to

$$i = \frac{9\pi e V}{64 k T} i_0 \frac{d^{3/4}}{(2C_s)^{1/4}}. \quad (17)$$

The procedure for obtaining a probe of true diameter d carrying maximum current (assuming that the only aberration of the probe-forming lens is the spherical aberration) is then as follows: (1) Adjust the Gaussian diameter of the probe to the value $3d/4$ (whatever the value of C_s), and (2) limit the aperture of the probe-forming lens to the value $u = (d/2C_s)^{1/4}$.

In practice, in order to avoid excessive wear of the filament, its temperature is set to the value $T = 2700^\circ\text{K}$, at which its emissive power is $i_0 = 2$

amp/cm². As a result the theoretical brightness of the crossover, for an accelerating voltage $V = 30$ kv, is $B = 82,000$ amp/cm² · steradian.

2. *Attempts to Obtain the Theoretical Brightness.* It must be noted that the theoretical value of B , which has just been calculated, is the maximum value of the brightness at the center of the crossover; Haine and Einstein (15) have shown that it was possible, under optimum operating conditions, to approach closely this theoretical value. On the other hand, if the probe is obtained by forming the image of the over-all crossover, as was the case in the first experimental instrument built by the author (2), the brightness which has to be inserted in the formulas is an average brightness. This value is much lower (the brightness decreases exponentially at the edges of the crossover) and it is necessary to introduce the notion of "gun efficiency" (2, 10). This efficiency is nothing more than the ratio of the mean value of the brightness of the crossover over its "whole surface area" (i.e. over the area where the brightness is noticeable) to the maximum value of this brightness at the center, and is about 7-10%. If it is required to obtain in the probe a current as close as possible to the theoretical maximum, it is necessary to eliminate the peripheral area of the crossover, by means of a limiting aperture, and to retain only its central part where the brightness is a maximum. This amounts to replacing the natural exit pupil, which the crossover constitutes for the electron gun, by a physical exit pupil of smaller diameter.

The gun model of Bricka and Bruck is particularly well suited to this operation, as the beam shows a crossover a few millimeters below the anode aperture, in a region of zero field. All that is necessary is to place at that level a platinum aperture whose diameter, of the order of 0.1 mm, is rather less than the half-diameter of the cross-over and which therefore eliminates all those parts of the crossover where brightness is less than about 60% of the maximum.

If a second aperture of small diameter (0.1 mm) is then placed in the path of the beam, all that need be done is to measure the electron current passing through the two successive apertures in order to deduce, knowing the distance and the diameters of the apertures, the brightness of the beam. The author was able to obtain, for a beam accelerating voltage of 30 kv and a cathode emissivity $i_0 = 2$ amp/cm², an average brightness $B = 58,000$ amp/cm² · steradian, or 70% of maximum theoretical value.

3. *Measurement of Probe Diameter.* Since the diameter of the electron probe is one of the main determining factors for the resolving power of the analysis, it is important to know it accurately. Several procedures are available for the purpose.

The simplest and quickest method consists in measuring on the micro-

scope the diameter of the contamination spot² which is formed on the sample at the point of impact of the electron beam. This spot appears more or less rapidly depending on the nature of the object and on the bombardment current (16). For instance, a visible spot is obtained on a copper sample bombarded under normal conditions ($V = 20$ kv, i about $0.05 \mu\text{a}$, probe diameter 0.5μ) after a 20-sec bombardment, while it is necessary to wait several minutes, under the same bombardment conditions, for the contamination spot to appear on a chromium sample.

The contamination spot tends to spread for a prolonged bombardment, with the result that the diameter measured on the microscope is greater than the true diameter of the probe. The relative error may become large with small diameter probes. To take an example, it can be noted that the contamination spot formed on a copper sample with a $1\text{-}\mu$ probe (even for a short-time bombardment) reaches a diameter of about 1.5μ . This method cannot be considered to be a precision method; in particular it is quite inadequate for verifying that maximum theoretical current has been obtained in the probe.

A second method consists in cutting off the probe by means of a sharp-edged metal strip (1) and observing on a fluorescent screen the shadow of that edge, considerably distorted by the spherical aberration of the reducing lens. The beam is then moved at right angles to the metal edge by means of an electrostatic or magnetic deflecting arrangement; calibration of the deflector allows the probe's minimum movement between the appearance of the shadow and the complete occultation of the beam to be determined. This arrangement provides means for easy adjustment of the probe on the sharp edge, this adjustment being obtained when the sharp edge cuts the beam in the neighborhood of the circle of least confusion. If the astigmatism of the reducing lens has been corrected previously, the adjustment criterion is very simple. With the metal edge located, say, to the left of the observer, the shadow should appear simultaneously at the extreme left of the field and at a spot situated at the right-hand side of the field, at three-quarters of its diameter (Fig. 7); the two shadows should then join up in a perfectly symmetrical manner. This procedure is an excellent test of the correction of astigmatism (2, 17).

This method is extremely simple if the instrument is normally provided with a probe deflection arrangement; all it requires is the insertion of a sharp-edged metal strip. This strip should previously be sharpened by electropolishing followed by ionic bombardment to eliminate impurity layers, for, if the edge is not perfectly clean and conducting, charging up may cause probe deflection. The amount of additional deflection varies during occulta-

² See Sec. II, C.

tion, and the exact deflection of the probe is no longer that which is deduced from the calibration of the deflector system. This additional deflection introduces some inaccuracy in the measurement of the probe diameter.

For accurate measurements, it seems preferable to use a third method (2) which consists in occulting the probe with a wire of known diameter. Suppose for instance that a probe is required with a diameter of $1\text{ }\mu$ and carrying, for a given accelerating voltage, maximum electron current. First, an aperture diameter is chosen for the probe-forming lens leading to the optimum value $u = (d/2C_s)^{1/4}$; then a tungsten wire $1\text{ }\mu$ in diameter is

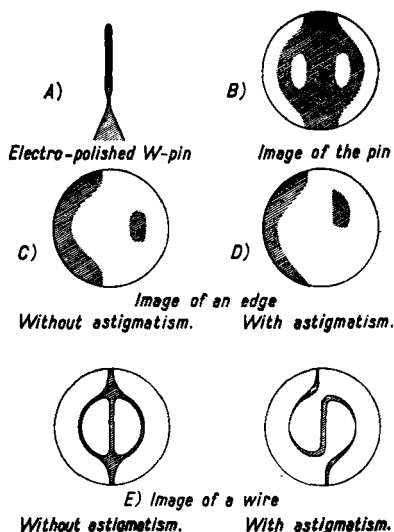


Fig. 7. Shadow microscopy images (Castaing and Descamps).

placed in the beam at right angles to its axis and the shadow of the wire is observed on the fluorescent screen placed in the lower part of the apparatus. The condenser is then strongly excited, so that the Gaussian diameter of the probe is very small, and the excitation of the probe-forming lens is adjusted so that the shadow of the wire covers the whole field. This complete occultation of the beam is easily obtained for if the astigmatism of the lens has been suitably corrected, the diameter of the probe is of the order of $0.25\text{ }\mu$. Then the beam current is gradually increased by reducing the condenser excitation until it is no longer possible to obtain complete occultation of the probe. The criterion for condenser excitation is as follows: With the wire properly centered in the beam, the excitation of the probe-forming lens is slightly modified; if the Gaussian diameter of the probe is too great (Fig. 7) two bright spots appear in the field, at one-quarter and at three-quarters of the diameter, before the periphery of the shadow has fully

covered the field. When the maximum Gaussian diameter compatible with complete occultation is obtained, a measurement is made, by means of a Faraday cylinder, of the current carried by the beam, which can then be compared with the theoretical value deduced from the emissivity of the filament and from the spherical aberration of the probe-forming lens.

In a typical experiment using a probe-forming lens with a spherical aberration coefficient $C_s = 3.6$ cm, an accelerating voltage of 30 kv and a tungsten wire 1.2μ in diameter, the author was able to verify that complete occultation of the probe was still obtainable for a beam current $i = 0.77 \mu\text{a}$. The theoretical maximum calculated from Eq. (17) is, for a probe 1.2μ in diameter, $i_{th} = 1.07 \mu\text{a}$. The efficiency of the probe-forming system is thus 72%. Naturally, such an efficiency can be attained only if the central part of the crossover alone is used for forming the probe. In the author's first experiments (2) in which the whole of the crossover was used, and in which, in addition, the spherical aberration coefficient of the probe-forming lens was 20 cm (electrostatic lens), the maximum current obtained on a $1\text{-}\mu$ probe was $0.015 \mu\text{a}$, or about 30 times less than in the present instrument ($0.47 \mu\text{a}$ on a $1\text{-}\mu$ probe). Such a current is much too great for the needs of spot analysis and it is possible to reduce the probe diameter to a value of about 0.4μ while retaining high enough an intensity.

When the probe current approaches its maximum value, the temperature of the tungsten wire used for occultation is raised to a considerable extent and mere radiation loss would not enable it to keep below its melting point. It is therefore necessary to arrange effective cooling by conduction. To this end, instead of a wire of uniform diameter, the end of a 0.1-mm wire is thinned down by electrolytic polishing. It is relatively easy to obtain the shape shown in Fig. 7 by this method. The diameter of the thinned-down part is measured, either with an electron microscope, or by shadow microscopy in the analyzer itself; the conical part is a very effective means for conducting the heat away; in spite of this, the thinned-down part, which can be observed during the experiment by means of the viewing device, is raised to white heat.

In order to obtain high efficiencies it may be necessary to effect prior correction of the astigmatism of the probe-forming lens; but correction does not need to be as carefully made as in the case of an electron microscope. It is only necessary that the residual astigmatism after correction be less than 1μ in order that it have no detectable effect on the probe diameter. Simple observation on the fluorescent screen of the shadow of a sharp edge allows the stigmator to be adjusted in a perfectly satisfactory manner. If, for special reasons (for example, in order to obtain a probe of very small diameter) a very carefully made correction for astigmatism is required, use can be made of the method proposed by the author (17). This technique

consists in observing on the fluorescent screen the shadow of a very fine diameter wire (diameter of the order of $0.01\ \mu$) placed at right angles to the beam axis at the level of the probe, i.e., a little above the Gaussian focus.

If the lens is perfectly corrected for astigmatism, this shadow for any orientation of the wire consists of the combination of a straight line and a circle (the circle corresponding to the cone of rays for which the aperture u is such that the focus F_u is on the wire). A similar image is obtained with an astigmatic lens when the direction of the wire coincides with that of one of the focal lines; if such is not the case, the appearance of the shadow is asymmetric (see Fig. 7). In particular, if the wire is set at 45° to the focal lines, the image obtained provides immediate means for determining the value of the astigmatism by a very simple geometric construction (2, 17).

In order to obtain perfect correction for astigmatism, the procedure is then as follows: A ring which carries a large number of wires set out in all directions is inserted in the beam. It is convenient to use plexiglass wires prepared from a solution of plexiglass in aniline and then coated with chromium by vacuum deposition. Note is taken of one of the wire orientations which produces the symmetrical circle-and-straight-line image (direction of one of the focal lines); a wire is then chosen whose orientation is at 45° to that direction and the stigmator is adjusted to produce a symmetrical image. Correction is complete when the symmetrical image is obtained for any orientation of the wire. This operation takes only a few minutes and ensures a reduction of residual astigmatism to less than $0.5\ \mu$.

4. *Possibility of Improving the Probe Brightness.* Further on it will be seen that probe brightness is one of the main factors which limit the resolving power in electron probe microanalysis. Higher electron densities would be useful for the analysis of very light elements, such as carbon, and it would be extremely valuable in high-resolution analysis of thin films.³ Two processes can then be considered for increasing the brightness of the probe.

a. *Use of a field emission cathode.* Marton (18) has suggested that the use of a field emitter (a tungsten point, for instance) could increase the current density in a probe of a given diameter, and experiments on such cathodes have been carried out at the National Bureau of Standards. Use of a pulsed field emission has also been investigated by Wittry (19). In good agreement with the calculations of Cosslett and Haine (20), Wittry reaches the conclusion that field emission is preferable to classical thermionic emission as soon as the diameter of the probe required is less than about $0.1\ \mu$, the ordinary hot cathode giving a higher density for probes of a larger diameter. It therefore appears that field emission would be of value only for the high-resolution analysis of thin films. Serious technical difficulties will have to be overcome in order to obtain a sufficiently stable emission for long time operation. It

³ See Sec. II, E, 3.

would seem that best results are obtainable from the use of thermionic field emission (21). This technique consists in heating the emitting point to a temperature slightly below that which corresponds to thermionic emission, and then applying the extractor field in the form of very short pulses (1 μ sec). This source shows fair stability under the relatively high residual pressures which cannot be avoided in an electron probe microanalyzer; unfortunately, in the present state of technique, the life of such cathodes is hardly more than 1 hr.

b. Correction of the spherical aberration of the probe-forming lens. A less revolutionary solution, but probably more practical, consists in reducing or even in trying to correct completely the spherical aberration of the probe-forming lens, which enters at the two-thirds power in the expression for maximum electron current attainable in a probe of a given diameter [Eq. (17)]. It is well known that the reduction of C_s in a lens with axial symmetry can be obtained only by reducing the focal length; such an improvement of C_s is achieved in Duncumb's and Melford's instrument (22) at the expense of the X-ray spectrometer resolution for the probe is formed inside the lens⁴ and the closest the crystal can be moved to the specimen is about 15 cm, necessitating a spectrometer of the semifocusing type.

Archard (23) has proposed the use of spherical aberration correction devices, originally designed for electron microscopy (magnetic quadrupoles and octupoles), in electron probe systems. This does appear to be the best solution, and spherical aberration correction seems likely to find an easier field of application in electron probe systems than in high-resolution electron microscopy.

In the present state of technique, the minimum value of the spherical aberration coefficient is about 0.03 cm (24) for an axially symmetrical lens. We shall call "ideal probe" one obtained with such a lens associated with a perfect hot cathode gun, as opposed to the probe—which will be referred to as "long-focus probe"—obtained experimentally by the author by means of a relatively long-focus lens, the gun efficiency being 72%.

Assuming for both cases a cathode emissivity of 2 amp/cm² and a cathode temperature of 2700°K, we obtain from Eq. (17) the following expressions for the current carried by a probe of diameter d , at an accelerating voltage V :

$$i = 0.535 V d^{3/4} \quad (\text{ideal probe conditions}) \quad (18)$$

$$i = 0.0158 V d^{3/4} \quad (\text{long-focus probe conditions}) \quad (19)$$

where i is expressed in microamperes, V in kilovolts, and d in microns.

5. Automatic Regulation of Probe Current. The fundamental operation of the analysis consists in comparing the intensities of one characteristic

⁴ See Fig. 15.

radiation in two successive measurements in which the sample and the reference target in turn are subjected to the same electron bombardment conditions. Sometimes many points of the sample are analyzed in succession (this is the case, for instance, in the determination of intermetallic diffusion curves) and the intensities emitted by the various points analyzed are all compared to the intensity emitted by the pure metal, the latter being measured once for all. In this way each analysis requires only one measurement instead of two, which is an appreciable saving of time. It is

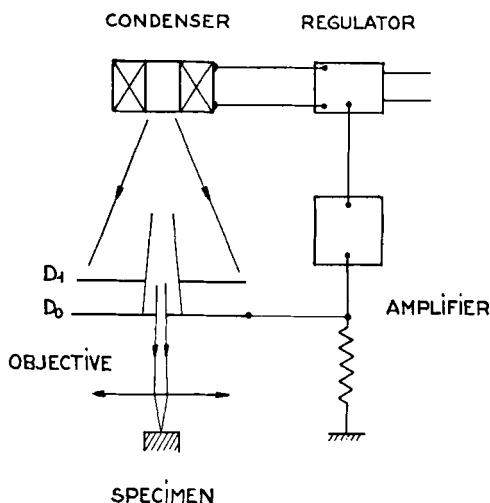


FIG. 8. Probe current regulating system (Castaing and Descamps).

then important that the electron current carried by the probe remain rigorously constant over the whole period of the measurements, to the same extent as the beam accelerating voltage and the adjustment of the spectrometer. But it may happen that the gun emission is subject to a slight drift in the course of measurements made over a long period; this drift is due mainly to an off-centering of the tungsten filament.

Figure 8 shows the arrangement of an automatic regulation system (25) which makes the probe electron current practically independent of any variation in the total gun emission. The aperture D_0 of the probe-forming lens is preceded by a coaxial aperture D_1 with a diameter k times as great. Since the electron density in the plane of aperture D_1 is uniform around the center, the aperture D_0 receives an electron bombardment of intensity I proportional to the current i carried by the probe, the proportionality coefficient being $k^2 - 1$. A constant fraction r of this intensity I is diffused back; as a result, if the aperture D_0 is connected to earth through a high resistance

R , the current through to this resistance is $I(1 - r)$, and hence the potential difference developed at its terminals is proportional to the current i , the proportionality coefficient being $R(1 - r)(k^2 - 1)$. All that is then necessary is to control the excitation of the condenser by this potential difference by means of an electronic arrangement in order to obtain an excellent regulation of the current i carried by the probe. The regulation may be sufficiently effective to ensure that a two-to-one variation in the total gun emission does not bring about a variation greater than 1% in the electron current of the probe.

Another method would consist in regulating the electron current absorbed by the sample in accordance with Wittry's suggestion (19). This current may differ considerably from the probe current through back-scattering effects and the author feels that such a procedure would present several disadvantages:

First, emission concentration proportionality is no longer valid in this case, and this introduces a serious complication as well as some uncertainty in the interpretation of the results.⁵ Also, it would be rather difficult, in scanning analysis for instance,⁶ to cause the probe to adjust its current without any delay to the rapid changes which would be involved by a sudden move from a low scattering point on the sample to an adjacent point where back-scattering is strong. In this case, the procedure of controlling by means of the condenser, whose inductance is quite large, would be difficult to apply.

B. Thermal Conditions of the Analysis

The electron density in the region of the sample bombarded by the probe is distinctly greater than that on the anticathode of a usual X-ray tube; it might therefore be feared a priori that the sample might become seriously overheated at the analyzed point. This is, in fact, not the case since the very small diameter of the bombarded region permits very strong cooling by thermal conduction.

The temperature rise in the center of the probe has been calculated by the author (2) for the case of a massive hemispherical sample (the external shape of the sample has practically no effect on the result) with its outer surface kept at room temperature. Electronic bombardment brings a uniform amount of power into a hemisphere whose radius r_0 is taken as being equal to that of the probe (it is actually greater, and so the calculated temperature rise is overestimated). Under these conditions maximum temperature rise at the center of the probe is

⁵ See Sec. III, *F*.

⁶ See Sec. II, *E, 1, c*.

$$\theta_m = \frac{W_0}{4\pi JC} \left(\frac{3}{r_0} - \frac{2}{R} \right) = \frac{3W_0}{4\pi JC r_0}, \quad (20)$$

where R is the radius of the sample ($R \gg r_0$), J is the mechanical equivalent of heat, C is the thermal conductivity of the sample, and W_0 is the power carried by the beam (which we suppose entirely converted into heat).

In the case of a metallic sample, the temperature rise obtained in this way is quite negligible. For example, under the impact of a probe 1μ in diameter carrying a maximum current of $0.47 \mu\text{a}$ at 30 kv the temperature rise of a copper sample would be less than 18° . Such is not the case, however, if the sample analyzed is a thermal insulator, and, under these conditions, one often observes thermal effects at the bombarded point when the low proportion of the constituent analyzed requires the use of a high electron current. Such samples can be coated with a thin conducting film (metal layer or carbon coating) with the double purpose of evacuating the heat dissipated in the sample and of holding the surface of the sample at constant potential by removing electrostatic charges.

It is also of interest to examine what goes on when a thin sample is penetrated by the beam electrons (high resolution analysis by transmission); for it is in this case that it becomes necessary to use the highest possible electron density. In the case of a thin layer of thickness e , cooled over a circle of radius R , and bombarded at its center by an electron probe of radius r_0 , it is found (2) that maximum temperature rise at the center is

$$\theta_m = \frac{W}{4\pi JCe} \left(1 + 2 \ln \frac{R}{r_0} \right), \quad (21)$$

where W is the power absorbed by the sample. As long as e is small compared to the maximum path of the electrons, W is practically given by the relation $W = \sigma \rho e W_0$, where W_0 is the power carried by the beam, ρ is the specific weight of the sample, and σ is the Lenard's absorption coefficient. Then

$$\theta_m = \frac{W_0 \sigma \rho}{4\pi JC} \left(1 + 2 \ln \frac{R}{r_0} \right), \quad (22)$$

σ is of the order of 10^8 for an accelerating voltage of 40 kv (26) and would be much less at the high accelerating voltages which would have to be used for high-resolution transmission analysis.⁷ Therefore the temperature rise would be considerable in probes of large diameter carrying large electron currents. This is the case of the temperature rise, in the electron microscope, of samples sufficiently thick to ensure that radiation loss is small compared to conduction loss. But analysis of thin layers will necessarily require the

⁷ See Sec. II, E, 3.

use of probes of very small diameter. Since W_0 varies as the 8/3 power of the diameter of the probe and since the logarithmic term varies only slowly, the temperature rise will decrease with the decreasing size of the probe.

Let us take for example the case of an "ideal probe" (Eq. 18) 0.1μ in diameter, carrying a current of $0.046 \mu\text{a}$ at an accelerating voltage of 40 kv and impinging on a thin copper sample. The rise of temperature at the center of the point of impact is of the order of only 7° . Even if it is assumed that the spherical aberration correction of the probe-forming lens can bring the diameter of the probe to 0.01μ while retaining its current value (the solid angle of the probe-forming beam would have to be greater than 0.5 steradian in the case of a hot cathode gun!), the temperature rise at the point of impact would increase from 7 to 9° . It is therefore certain that thermal limitations will in no way hinder the securing of high resolution in the analysis of thin layers by X-ray spectrography.

C. Contamination

It is well known that a sample subjected to electron bombardment in a dynamic vacuum gradually becomes covered with a "contamination" layer due to polymerization, under the action of the beam, of organic matter adsorbed on the surface. Ennos (27) has shown that organic molecules condense directly on the sample from vapors present in the enclosure. To this phenomenon there is added, in the case of a highly localized bombardment, a superficial migration towards the bombarded point of organic matter condensed on the surface as a whole (16). Ennos found that heating the sample to 250°C or surrounding it with a cold trap effectively reduced the contamination rate. Unfortunately, heating the sample is not always acceptable; certain alloys, for instance, are liable to suffer a transformation at a relatively low temperature. Also, the installation of a cold trap raises some practical difficulties, and the necessity of providing clearances for the exit path of X-rays lowers its efficacy. Castaing and Descamps (16) have shown that it is possible, not only to lower the contamination rate but also to remove pre-existing deposits by means of a low-pressure air jet directed onto the region bombarded by the beam. However, this solution, as pointed out by Wittry (19), has two undesirable effects: as a result of operating the beam at higher pressures, filament life is reduced and the contamination rate in other parts of the beam system is increased because of greater back diffusion of vapors from the pump.

The effect of the contamination is not very troublesome so long as the accelerating voltage used for the beam is much greater than the critical excitation voltage of the line analyzed. Such is not the case if, with the object of increasing the resolving power,⁸ a low accelerating voltage is

⁸ See Sec. II, E, 2.

chosen; in this case it is essential to eliminate contamination completely. Consideration of Eq. (23) shows, for example, that, in the case of the analysis of copper by means of an accelerating voltage of 10 kv, the presence of a contamination layer only 200 Å thick (in the absence of special arrangements such a layer is formed in a few seconds) suffices to lower the energy of the incident electrons by some 70 ev and to reduce the emission of Cu $K\alpha_1$ line by more than 10%.

D. X-ray Recording

1. *Conditions to be Satisfied.* X radiation emitted by the sample consists, in addition to the characteristic radiations of the various constituents of the bombarded region, of a continuous background which increases as the mean atomic number of the bombarded point increases. Therefore the analyzing device for this radiation has to satisfy the two essential conditions:

(1) High sensitivity, as the intensity of the X-rays is relatively low. The electron current used for the excitation being of the order of $0.1 \mu\text{a}$, the X-ray emission of the sample is about 100,000 times less than that of an ordinary X-ray tube and the detection technique necessarily uses a counter capable of recording the individual X photons. This detector may be a GM counter, scintillation counter, or proportional counter. The counter is generally preceded by a bent crystal monochromator, the whole making up a conventional X-ray spectrometer. In order to give some idea of the experimental conditions, we shall just indicate that the impact of a $0.33\text{-}\mu$ probe, carrying an electron current of $0.025 \mu\text{a}$ at an accelerating voltage of 30 kv, on a pure copper block gives rise to a Cu $K\alpha_1$ emission which, when measured in a bent quartz spectrometer and a GM counter, reaches 1,500 counts/sec. Such an intensity is adequate for a rapid and accurate measurement of the characteristic emissions.

(2) Good discrimination; it would seem a priori that the extreme simplicity of the spectra would not require the use of a highly dispersive instrument for isolating the characteristic lines, and, in fact, quite a coarse discrimination is sufficient for isolating the K spectra of the various elements. This is no longer true when using the L spectra, which is essential in the case of heavy elements for which the excitation of the K levels would demand an electron accelerating voltage incompatible with correct localization of the analysis. The L spectra have many more lines, and it is obviously important that they be perfectly separated by the spectrometer to avoid all risk of ambiguity between separate elements.

But the usefulness of high discrimination arises mainly from the fact that the limit of detection of the analysis (minimum detectable concen-

tration) is lowered as the discrimination of the spectrometer increases as a consequence of improved signal-to-noise ratio.

2. *Practical Designs.* In the French model (25) analysis of X radiation is effected by means of two similar spectrometers, the crystals and the counters rotating over the same focusing circle (Rowland circle) of 25-cm radius (Fig. 9a). A gear system gives the counter a speed of rotation which

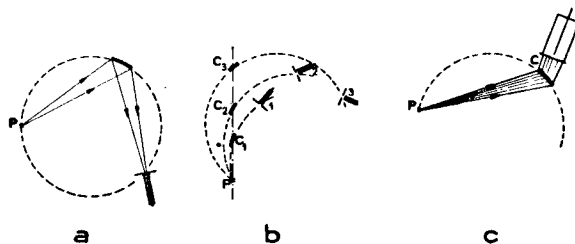


FIG. 9. Three spectrometer arrangements.

is twice that of the crystal. The radiations reflected by the crystal thus come, whatever the angular position chosen and hence the reflected wavelength, to a focus exactly at the center of the counter input window. A dial graduated in degrees and minutes shows continually the angle of incidence of the X-ray beam on the crystal and hence the wavelength of the reflected rays.

a. *Usual wavelengths.* One of these spectrometers is used to detect radiation of medium wavelength in the band 0.6 to 4.5 Å, and so it permits the analysis by *K* lines of all elements situated in the periodic table between chlorine and molybdenum, and the analysis by *L* lines of all elements heavier than molybdenum. The detector is a GM counter with a mica window and the crystal is a quartz plate 0.3 mm thick of the Johannson type (ground and bent). A similar arrangement is used in many other instruments (11, 12), the quartz crystal often being replaced by a lithium fluoride crystal. Lithium fluoride gives a broader reflection, which could be an advantage if the spectrum as a whole were recorded by a scanning method, because the integrated intensity reflected by the lithium fluoride is in this case much greater than that reflected by a quartz crystal under the same conditions. But microanalysis is a case of a method of analysis in which we have to consider peak intensity and not integrated intensity. Peak intensity is practically as great for a quartz crystal (provided the crystal is correctly curved and the spectrometer is well adjusted) as for a lithium fluoride crystal, with the considerable advantage that the discrimination—and consequently the signal-to-background ratio—is much better in the case of the quartz. The bent quartz spectrometer provides means for

the convenient separation of the two components of the $K\alpha$ doublet for elements of medium atomic number. This possibility is of no particular interest in itself for the analysis, but this resolution is related to the ability to achieve a value of the signal-to-continuous background contrast which is of the order of 400 when pure elements are bombarded. This observed signal-to-continuous background contrast is in good agreement with Cambou's measurements (28) in which he used the method of Ross's double filters and a beam accelerating voltage of 30 kv. It can be deduced directly from Cambou's results that the portion of continuous spectrum emitted between the absorption limits Cu K and Ni K ($\Delta\lambda = 0.1065\text{\AA}$) by a pure zinc anticathode has an intensity equal to 18% of the intensity emitted in the Zn $K\alpha$ doublet. As a result, for a spectrometer whose discrimination is just sufficient to separate the two components of the doublet ($\Delta\lambda = 0.00386\text{ \AA}$), the signal-to-continuous background contrast is, when the spectrometer is adjusted to the Zn $K\alpha_1$ line which carries two-thirds of the $K\alpha$ intensity,

$$Q = \frac{2}{3} \frac{0.1065}{0.18 \times 0.00386} = 100,$$

neglecting the self-background of the counter, which is mainly due to cosmic rays and amounts to about 30 counts/min.

The value of 400 obtained for the line-to-continuous background contrast permits very low concentrations to be detected; an iron concentration of 0.02%, for instance, is very easily detected since the Fe $K\alpha_1$ line projects above the continuous spectrum by nearly 10%.

Other types of spectrometers are also used. Borovsky (29), in an apparatus designed in 1953 independently of the previous work of the author, uses a bent crystal operating by transmission (Fig. 9c) which naturally is applicable only for relatively hard lines. Figure 9b shows the arrangement used by Fisher (30), in which the reflecting crystal moves in a straight line from the source and so constantly sees the source in the same direction. Some authors also use a plane crystal whose effectiveness, however, is less than that of the bent crystal. Last, Birks and Brooks (31) set up several crystals and fixed detectors for the simultaneous analysis of several elements (system analogous to that of the quantometer) which has the advantage of reducing the time required for the analysis on a given point of the sample and consequently the degree of its contamination by the beam.

b. Light elements. The analysis of light elements is made rather more difficult by the fact that their characteristic radiation is much softer and hence easily absorbed. We shall here describe the soft radiation spectrometer used in the French model (25) which enables the waveband from 4 Å to 12 Å to be analyzed.

The reflecting crystal is a mica strip curved on a 50-cm radius; the receiver is a proportional counter with gas flow (Fig. 10). The window of this counter consists of a 6- μ Mylar foil whose absorption is only 40% for a radiation as soft as Si $K\alpha$ (7.11 Å). The Mylar is somewhat permeable to water vapor, and this prevents the design of a sealed-off counter; gas flow has therefore to be used, the rate of flow of the gaseous mixture (90% argon and 10% methane) being about 10 cm³/min. The lateral arrangement of the window makes it possible to avoid any blind space; the drop in sensitivity of the counter at the longer wavelengths then arises only from the absorption in the window, which is slight up to 10 Å. A bypass arrangement (Fig. 11) enables the counter to be evacuated before the gas is introduced.

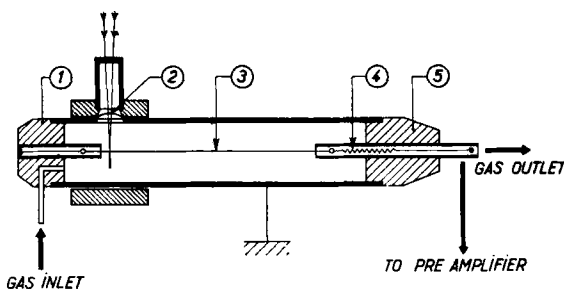


Fig. 10. Proportional counter (soft X-rays) (Castaing and Descamps). 1. Araldite (a trade name for an epoxy resin); 2. Window (Mylar 6 μ thick); 3. Tungsten wire (20 μ diameter); 4. Wire tension spring; 5. Araldite.

This arrangement avoids the long flowing process which would otherwise be necessary to eliminate completely the inside air, and the counter is ready for operation in less than 5 min. The constancy of the gas flow is secured by a capillary; the gas pressure is slightly above 1 atm, avoiding contamination by air. The small diameter (20 μ) of the central tungsten wire enables the operating voltage to be lowered to 1500 v. A preamplifier located in the evacuated space of the spectrometer follows the counter in its motion.

To take an example, it may be mentioned that the Si $K\alpha$ line emitted by a block of pure silicon under an electron bombardment of 0.1 μ a at 15 kv gives an intensity of 1000 counts/sec, the signal-to-background ratio being about 100, which is sufficient for a quick and accurate measurement. It is, of course, necessary to evacuate the spectrometer in order to record such soft lines (the introduction of atmospheric air in the spectrometer would lower the intensity of the Si $K\alpha$ line in the ratio of 10¹³). In order to avoid the presence of an absorbent window between the source and the crystal, a secondary vacuum is applied in the spectrometer, and the outlet

spectrum. But it should be noted that one of the cases where it will be essential to use large-aperture beams and nondispersive detector systems is high-resolution analysis of thin layers⁹ where such absorption is negligible; hence this happy consequence that the main disadvantage of the double-filter method vanishes in one of the cases for which a large collection efficiency becomes essential.

d. Special design. Riggs (34) has designed an arrangement which makes it possible to keep the specimen in air outside the electron optics system. A 10- μ hole through a mica sheet allows the electron probe to emerge and strike the surface of the sample. Emitted X-rays which leave the surface at a take-off angle of 55° first pass back through the mica sheet and then emerge again through a beryllium window; excessive air leakage through the 10- μ hole into the electron optical system is prevented by an auxiliary pumping path near the window.

With Riggs's instrument, specimens weighing several hundred pounds may be examined; this is of particular interest in the analysis of big meteorites.

e. Possibility of extension to very light elements. The extension of the analysis to very light elements, such as carbon introduces quite serious difficulties. The characteristic lines are of very long wavelength (44 Å for carbon) and therefore easily absorbed. Moreover, the efficiency of the dispersive systems which can be used in this wavelength region (ruled gratings for instance) is very bad (11).

Dolby and Cosslett (35) have undertaken a detailed examination of the possibility of using nondispersive systems for the separation of characteristic lines in this region, and the results they have obtained are very encouraging.

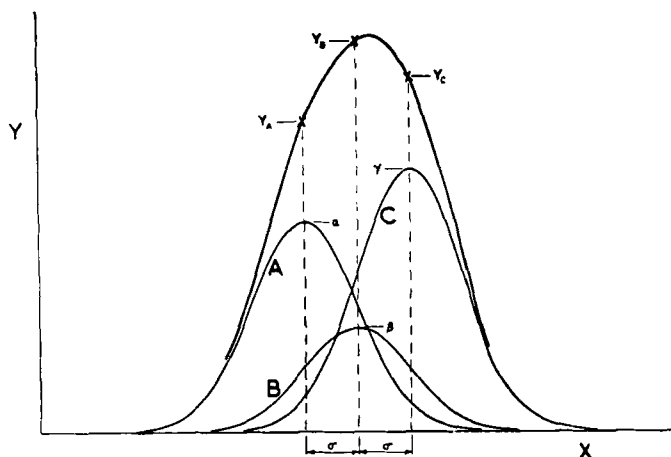
They start from the observation that "high efficiency is necessary to keep the beam voltage and current as low as possible, both from specimen heating and spatial resolution considerations. The quantum efficiency problem is particularly acute when scanning images¹⁰ are desired. The best available energy discriminating detector having high collection efficiency is the proportional counter. However, proportional counters do not have sufficient energy resolution for separating the *K* X-ray lines of elements closer than about three in atomic number. But the collection efficiency overrides this disadvantage" and the authors have centered their effort around the direct use of a proportional counter followed by a special pulse analysis method which overcomes many of the problems associated with low-energy resolution.

This "matrix method" is illustrated in Fig. 12. The three overlapping

⁹ See Sec. II, E, 3.

¹⁰ See Sec. II, E, 1, c.

pulse height distributions from elements A, B, and C, adjacent in the periodic table, add together to give the composite curve Y ; this last curve is known from the experimental measurement, but the constituent amplitudes α , β , and γ are unknown. These amplitudes can then be found by expressing three ordinate measurements Y_A , Y_B , Y_C in terms of the component amplitudes and solving the three equations for α , β , and γ . The coefficients evidently depend on the exact shape of the constituent curves, which may be known from experiments on pure elements. The values chosen



Measurements

$$Y_A = \alpha + 0.607\beta + 0.135\gamma$$

$$Y = 0.607\alpha + \beta + 0.607\gamma$$

$$Y_C = 0.135\alpha + 0.607\beta + \gamma$$

Solutions

$$\alpha = 1.83Y_A - 1.52Y + 0.68Y_C$$

$$\beta = -1.52Y_A + 2.85Y + 1.52Y_C$$

$$\gamma = 0.68Y_A - 1.52Y + 1.83Y_C$$

FIG. 12. A composite curve and its constituent curves A, B, and C (by courtesy of R. M. Dolby and V. E. Cosslett).

in the example (Fig. 12) correspond to Gaussian distributions with the same standard deviation, and peaks separated by a distance equal to this standard deviation. Electronic mixing of the outputs with the appropriate signs (Fig. 13) makes it possible to solve the equations automatically; ordinate measurements are replaced by area measurements (vertical strips) performed by three identical pulse analysis channels.

The method could be applied to the separation of the characteristic lines of carbon, nitrogen, and oxygen; however, absorption in the inlet window makes it rather difficult, for the moment, to design proportional counters recording efficiently the nitrogen and oxygen lines. Meanwhile the authors have applied the method to the separation of magnesium, aluminum, and silicon lines with excellent results.

The only disadvantage of this method lies in the fact that it increases the influence of statistical fluctuations on the accuracy of the results; statistical errors of 5% in the determination of the ordinates Y_A , Y_B , Y_C cause, for instance, in the β amplitude (Fig. 12) an error of about 30%. In practice this amounts to lowering the collection efficiency of the counter by a factor of about 40. Nevertheless, this method seems to hold out a real hope for the microanalysis of very light elements, at least in the absence of heavy constituents whose L spectrum would seriously complicate the situation.

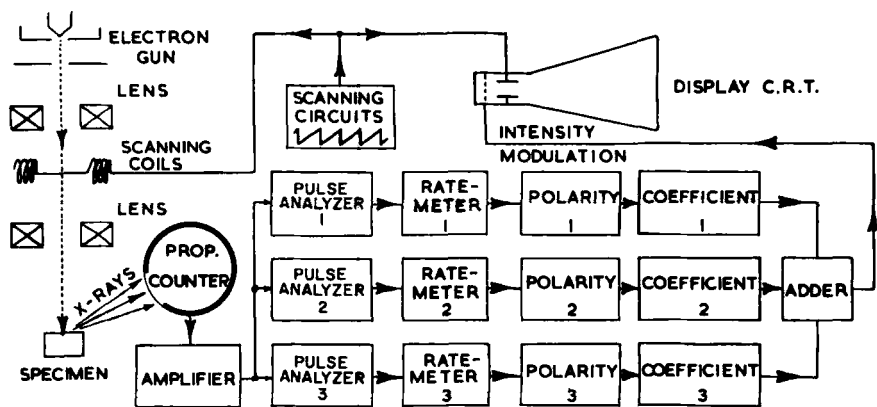


FIG. 13. Scanning X-ray microanalyzer incorporating the matrix method of pulse analysis (by courtesy of R. M. Dolby and V. E. Cosslett).

But it must not be forgotten that, even if a satisfactory method for recording lines is developed, serious difficulties will remain for the practical application of the method to precision quantitative analysis, mainly as regards absorption correction.¹¹ In order to maintain self-absorption within acceptable limits, it will be necessary to use very low accelerating voltages (a few kilovolts), and the analysis will be extremely sensitive to the presence of surface impurities such as contamination.

E. Localization of the Analysis

1. Various Procedures for Localizing the Point of Impact of the Probe. The accurate determination of the point of impact of the probe is one of the main problems in electron probe microanalysis. This determination has to be effected with an accuracy at least equal to the discrimination of the analyzer, i.e. better than $1\ \mu$. The method most commonly used consists in observing the sample during the operation by means of a viewing device consisting of an optical microscope.

¹¹ See Sec. III, D.

a. Optical viewing of the sample. In the original apparatus developed by the author (2), the viewing device consisted of the object lens of an ordinary microscope, preceded by a mirror placed between the object and the probe-forming lens. The mirror had a hole 0.2 mm in diameter to let the electron beam through, and its orientation was such that the viewer's optical axis, perpendicular to the surface of the sample, was inclined at about 10° to the electron beam axis. This arrangement makes it possible to reject the shadow generated by the mirror orifice. A similar arrangement is at present used in several instruments; it has the disadvantage of limiting the numerical aperture of the viewing microscope used to about 0.25 and its resolving power to about 1.5μ . But the experimenter should be able to distinguish easily the structural details of a sample with which he is familiar from observation with excellent metallographic microscopes.

A perfectly satisfactory solution consists in observing directly the surface of the sample by means of an objective centered on the electron beam; a reflecting objective (36) was adopted in the French model (Fig. 5). The advantages of such an arrangement are many: The reflecting objective has a large working distance (about 17 mm) while retaining a large numerical aperture (0.48) and a resolving power of 0.7μ . In addition, the axial part of the objective plays no part in the formation of the image and so can conveniently be provided with a hole for the electron beam; the objective has no nonconducting surface liable to cause charging up effects; last, none of the optical surfaces is opposite and close to the point of impact of the probe. This last feature makes it possible to prevent contamination of the surfaces under the action of back-scattered electrons.

This objective is associated with a reticular eyepiece; it is only necessary to make a preliminary adjustment to cause a coincidence of the point of impact of the probe with the cross lines. This adjustment is effected by means of a small fluorescent screen set up permanently on the specimen holder. The position of the probe is therefore fixed in three dimensions because of the very small depth of field of the viewing microscope. The construction of the specimen holder makes it possible to bring in succession under the impact of the probe the point chosen for the analysis and the standard composed of the element to be assayed. A set of 42 standards composed of pure elements or definite compounds is permanently fixed on the specimen holder.

The exact position of the point of impact of the probe can be constantly verified by observing the contamination spot produced by a prolonged bombardment. It is thus possible to observe slight displacements of the probe which occur, in particular, when analyzing a highly magnetic sample. These displacements are then compensated for by means of the electrostatic device for deflecting the beam. It is important that the probe

always be in precisely the same position with respect to the spectrometer, at least when the latter uses a dispersive crystal of high discrimination.

b. Rotating drum. The arrangement developed by Mulvey (11) avoids the use of a reflecting objective and the difficulties involved in placing it on the axis of the probe-forming lens; the specimen is mounted on a drum and is rotated out of the electron beam in front of a regular microscope for viewing. In this way it is possible to observe the sample by means of an excellent metallographic objective with a resolving power close to $0.3\ \mu$. Also, the probe-forming lens does not have to be specially designed to accommodate the objective on its axis, hence a greater structural simplicity. But the difficulties are transferred to the design of the

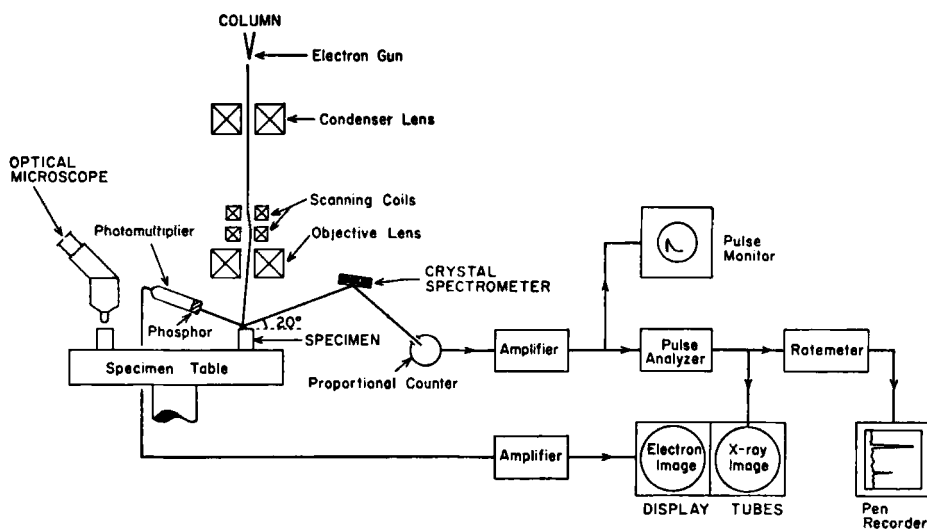


FIG. 14. Schematic diagram of the X-ray scanning microanalyzer (by courtesy of P. Duncumb and D. A. Melford).

rotating drum which has to ensure absolute correspondence between the point viewed by the microscope and that bombarded by the probe. It seems that a precision better than $1\ \mu$ can be held only with difficulty over a long period of routine operation. The scanning technique proposed by Cosslett and Duncumb enables this difficulty to be overcome.

c. Scanning analysis. Cosslett and Duncumb (37) have developed a scanning technique which permits rapid study of the surface distribution of the different elements. The electron probe is scanned over the specimen surface in synchronism with the spot of a cathode-ray tube whose brightness is modulated by a signal from the spectrometer detecting the characteristic emission of the selected element (Fig. 14).

The value of this method arises from the fact that it makes it possible to detect rapidly local variations of concentration (e.g. segregation) which often fail to appear on the image obtained on the optical microscope. Scanning hardly replaces the optical viewing method when a definite point of the sample (such as a precipitate) has to be rapidly brought under the impact of the probe in order to effect its quantitative analysis. According to Duncumb and Melford (22) "an image of the specimen surface showing the distribution of the element is obtained, and, after stopping the scan, the electron probe can be accurately positioned from the image afterglow for quantitative analysis." But it should be noted that a really accurate positioning is possible by this method only after the image has been established for a rather long time. If, for instance, a detail of the object (e.g. a precipitate), whose diameter is at the limit of resolution of the analyzer, i.e., $1\ \mu$, has to be centered under the impact of the probe, positioning has to be effected to a fraction of a micron. This centering requires that the resolution of the image be itself of the order of $1\ \mu$. Now the intensity recorded on the spectrometer is of the order of 10,000 counts/sec for pure elements and each surface element of one micron square must deliver at least some 20 counts in order that statistical fluctuations shall not completely mask the concentration fluctuations of the constituent to be assayed. Therefore the period required for establishing a sufficiently clear image of 0.4 mm side is of the order of 10 min, which necessitates the use of a very long remanence oscilloscope as a more complicated storage system.

Most fortunately, a more rapid view of the surface of the sample can be obtained by using the back-scattered electrons. In the Duncumb and Melford instrument, a scintillation counter is used to collect scattered electrons (Fig. 15) and the signal delivered by this counter is used to modulate the brightness of the oscilloscope. By this method image formation is considerably faster, the number of back-scattered electrons being 10^7 times greater than that of the X photons recorded on the spectrometer. But contrast in this case arises mainly from local variations of mean atomic number, and the examples of application given by the authors refer to samples in which these variations are large (e.g. aluminum-tin).

It is not yet certain that these two modes of observation are capable of completely replacing visual observation of the sample in the course of analysis by means of the metallographic microscope, at least if the method is to be capable of application to any type of sample. The ideal would be to combine direct vision on the metallographic microscope with mapping possibilities of the various elements by the scanning method developed by Cosslett and Duncumb. Electrostatic or magnetic scanning of the probe is, however, incompatible with the use of a high-resolution spectrometer. Displacement of the probe by a few hundredths of a millimeter completely

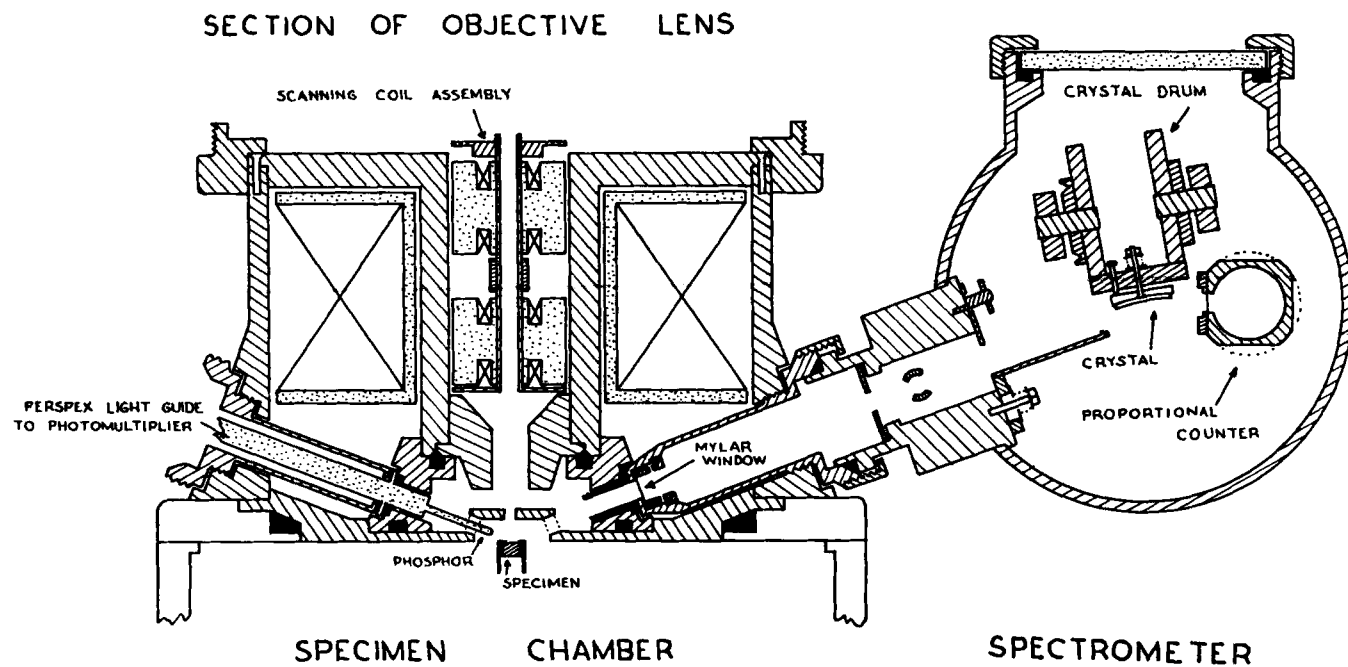


FIG. 15. The objective lens and X-ray spectrometer of the scanning microanalyzer (by courtesy of P. Duncumb and D. A. Melford).

upsets the adjustment of the spectrometer and falsifies the measured intensities. In Duncumb's and Melford's apparatus the crystal used (LiF) has a broad reflection, and this makes it possible to depart considerably from the strict focusing conditions; the disadvantage of this crystal is that the line-background contrast is low, which limits the possibilities of quantitative analysis in the region of weak concentrations. Considering that the period required for establishing a good X-ray image is in any case long, it is possible to replace the scanning of the probe by a mechanical scan of the sample itself, the probe remaining fixed. This allows the spectrometer to remain constantly focused on the X-ray source; in this way the advantages of scanning analysis can be combined with those of precision quantitative analysis.

2. *Limitation of Discrimination by Diffuse Penetration of Electrons.* In the course of their progress inside the sample, the electrons deviate from their initial direction; at the end of a travel which is shorter for a weaker accelerating voltage and for a higher atomic number of the bombarded region, the direction of the electron trajectory is no longer related to its initial direction and the penetration of the electrons in the sample is consequently completely diffuse. Some of the electrons may even be diffused back and leave the sample. As a result, the diameter of the region analyzed, i.e. the diameter of the sample region where the electrons still have sufficient energy to ionize the characteristic X-ray levels, is greater than the diameter of the probe itself. It is quite futile to use probes of very small diameter for the analysis if, at the same time, the precaution is not taken of lowering the accelerating voltage of the electron beam.

It is normal, in the usual X-ray tube technique, to use an accelerating voltage at least equal to three times the critical excitation voltage of the X level since it is well known that this gives the optimum value of the contrast between the characteristic emission and the continuous spectrum. If this rule is maintained in electron probe microanalysis, the voltage which will have to be used for assaying copper, for instance, is in the neighborhood of 30 kv. Under these conditions, the electrons follow, within the sample, a track of the order of $2\ \mu$ before their energy falls below the 9 kev which is necessary for the excitation of the K level of copper. Along this track, which obviously is not a straight line, the electrons depart from their initial trajectory by an amount which may reach about half the total path. As a result, the diameter of the region analyzed is greater by $2\ \mu$ than the diameter of the electron probe, and consequently there would be little point in seeking to improve the discrimination of the analyzer by reducing the diameter of the probe below $0.5\ \mu$.

But, as was shown by Wittry (38), it is not to be deduced that the resolution of the method is thus subject to a fundamental limitation and that

efforts to improve the probe brightness are of no interest. It is possible, if one wants to do away with the use of the best accelerating voltage for the excitation of X levels, to improve considerably the discriminating power of the analyzer, the only limit being, in fact, imposed by the performance of the probe-forming system (probe brightness) and the quality of the spectrometer used (line-continuous background contrast).

Wittry was able to establish the experimental conditions leading to optimum discrimination, on the basis of the observation that the volume or the diameter of the region analyzed may be made arbitrarily small by a suitable choice of the probe diameter and of the beam accelerating voltage; the only limitation is imposed by the necessity of obtaining a sufficiently accurate measurement of the line intensity without extending the measurements beyond a reasonable time. Without entering into the details of Wittry's calculations, the various stages of his argument can be summarized—with minor modifications—as follows:

First, the depth of the analyzed region can be estimated from Williams' law of deceleration modified, as suggested by Webster (9), by introducing the factor $2Z/A$. The equation obtained by Williams is applicable to relatively fast electrons ($\beta > 0.5$); here we shall modify slightly the numerical constant of Williams' equation (8) in order to adapt it to electrons with an energy between 10 and 30 kev; in good agreement with the results obtained by Williams on argon (39) and by Terrill on aluminum (40) we shall adopt the deceleration law

$$\frac{dV}{dx} = 1840\beta^{-1.4}\rho \frac{2Z}{A}, \quad (23)$$

where V is expressed in kilovolts and x in centimeters. It can be assumed that excitation at the maximum depth is produced by electrons which have suffered practically no deviation along their path. Writing that their deceleration has brought them from their initial energy $E = eV$ to the minimum energy necessary for exciting the K level (for instance) or $E_K = eV_K$, we obtain an approximate value of the depth of the analyzed region

$$z_m = 0.033(V^{1.7} - V_K^{1.7}) \frac{A}{\rho Z} \text{ microns}, \quad (24)$$

where V and V_K are expressed in kilovolts; A is the mean atomic mass of the bombarded point, Z is its mean atomic number, and ρ the local density in grams per cubic centimeter.

It can be assumed that the total diameter of the analyzed region is equal to

$$\delta = d + z_m, \quad (25)$$

where d is the diameter of the electron probe and z_m the maximum effective range.

The total diameter can, of course, be reduced indefinitely by reducing the diameter of the probe and lowering the accelerating voltage V to the immediate neighborhood of the threshold voltage V_K . But in this case the intensity of the line emitted by the sample becomes extremely weak and an accurate measurement of this intensity requires a very long time. For example, let us consider attaining an accuracy of 0.4% on the intensity emitted by the pure element by means of a measurement lasting no more than 1 min. If the intensity of the continuous background can be neglected compared to that of the characteristic line (which will be assumed in order to simplify calculations), the number of counts per second recorded by the counter should be $n = 500$ for the pure element.

But the intensity of the characteristic radiation is proportional to

(1) the electron current, i.e. to $Vd^{3/2}$,

(2) the efficiency of the electron-photon conversion, which is substantially proportional to $(V - V_K)^{1.6}$.

To take an example, let us consider the case of a pure copper sample ($V_K = 9$ kv) and a curved quartz spectrometer for which the intensity $\text{Cu } K\alpha_1$ is equal to 1500 counts/sec for an accelerating voltage $V = 30$ kv and a beam current of $0.025 \mu\text{a}$. These conditions result from Eq. (19) (long-focus probe conditions), for a probe diameter d and an accelerating voltage V , in an intensity of the $\text{Cu } K\alpha_1$ line of

$$I(\text{Cu}) = 7.3V(V - 9)^{1.6}d^{3/2}, \quad (26)$$

where V is expressed in kilovolts and d in microns.

The intensity of 500 counts/sec is thus obtained for a probe diameter

$$d = 4.74V^{-3/2}(V - 9)^{-0.6} \text{ microns.} \quad (27)$$

The application of Eq. (24) to the case of copper leads to the expression for the depth of penetration z_m

$$z_m = 0.0081(V^{1.7} - 42) \text{ microns.} \quad (28)$$

The diameter of the analyzed region, therefore, varies with the accelerating voltage used (the intensity of the $\text{Cu } K\alpha_1$ line being constantly held at 500 counts/sec) according to the relation

$$\delta = d + z_m = 4.74V^{-3/2}(V - 9)^{-0.6} + 0.0081(V^{1.7} - 42). \quad (29)$$

This expression gives a minimum for $V = 14.5$ kv; this gives the optimum conditions leading to the best discrimination when the line examined is the $\text{Cu } K\alpha_1$ line:

$$V = 14.5 \text{ kv; } i = 0.07 \mu\text{a; } d = 0.646 \mu; z_m = 0.421 \mu.$$

Under these conditions, the diameter and the volume of the analyzed region are

$$\delta = 1.07 \mu \quad \text{and} \quad v = 0.38 \mu^3. \quad (30)$$

For the ideal probe conditions [Eq. (18)] we would obtain the optimum values

$$V = 11.7 \text{ kv}; \delta = 0.475 \mu; v = 0.034 \mu^3. \quad (31)$$

We have assumed that the influence of the continuous spectrum is negligible; this is entirely justified in the case of a high-resolution spectrometer provided the concentration of the element being measured is not too small. In a more accurate calculation, Wittry (38) takes the continuous spectrum into account and reaches the following conclusions:

(1) The diameter of the analyzed region is a minimum for a rate of excitation V/V_K between 1.6 (strong concentrations for which the continuous spectrum is negligible) and 1.9 (low concentrations); however, this minimum is broad and slightly higher accelerating voltages may be used without reducing the linear discrimination markedly.

(2) The volume of the analyzed region has a much more sharply marked minimum for a rate of excitation V/V_K between 1.1 (strong concentrations) and 1.5 (low concentrations), minimum volume being in the neighborhood of $0.2 \mu^3$ in the case of pure copper.

The discrimination power can be even better in the case of the analysis of light elements for which the critical excitation energy of the X levels is in the neighborhood of 1 kev. Duncumb (41) obtains under these conditions a discrimination close to 0.1μ . His estimate is a little optimistic since the diameter of the analyzed region is obtained by a quadratic sum of the Gaussian diameter of the probe, of the diameter of the aberration disk, and of the maximum depth of excitation. This method certainly leads to an underestimation of the total diameter of the analyzed region. Considering only the first two terms, the intensity distribution in a probe whose Gaussian diameter is infinitely small shows a marked maximum at the edges, so that the optimum probe has a sharp edge intensity distribution.

In order to improve the discrimination in the case of elements of medium atomic number, Duncumb (41) recommends the use of very soft lines (L spectrum in the case of copper, M spectrum in the case of heavy elements). However, in addition to increased experimental difficulties, the use of the L or M spectra makes the estimation of fluorescence correction¹² a more delicate matter, and it seems preferable, in the case of a precision quantitative analysis, to limit ourselves to the K spectrum up to atomic number $Z = 35$ and to the L spectrum for the heavy elements.

¹² See Sec. III, E.

But it is nevertheless valuable to use for the analysis a relatively weak accelerating voltage exceeding only by 50 to 80% the critical excitation voltage of the element to be analyzed. The resulting gain in discrimination is particularly important when a relatively heavy element has to be measured in a sample of low density. Suppose, for example, that copper is the element to be measured in an aluminum-copper alloy of low copper content and of density around 2.7. With the electron current such that the pure copper emission is equal to 500 counts/sec we find the optimum conditions $V = 12.2$ kv, $d = 0.953$ μ , $z_m = 0.712$ μ or a discrimination $\delta = 1.7$ μ , the volume of the analyzed region being of the order of 0.5 μ^3 . The use of an accelerating voltage of 30 kv would make the diameter of the analyzed region greater than 7 μ , and its volume greater than 300 μ^3 !

The use of low accelerating voltages has the further advantage of reducing the magnitude of the absorption correction,¹³ but it has the disadvantage of increasing the thermal load of the sample, which is not too troublesome in the case of metal samples but could cause an unacceptable temperature rise in the analysis of thermal insulators.

Another disadvantage arises from the increased relative importance of fluorescence secondary emission excited by the continuous spectrum.¹⁴ However, it is possible that the ratio I_f/I which begins to grow when the excitation rate V/V_K passes from 3 to 2 (this effect is due to the increase in the average absorption of the continuous spectrum in the sample), decreases again when the excitation rate approaches unity. This behavior results because the intensity of the exciting continuous spectrum decreases as $(V - V_K)^2$ while the intensity of the line excited by direct ionization decreases as $(V - V_K)^{1.6}$.

Last, a practical disadvantage is the fact that the improvement in the discrimination is obtained mainly by a reduction of the maximum penetration of the electrons in the sample; the analysis thus becomes more superficial in character and the influence of the surface state of the sample becomes a dominant feature. Unfortunately, chemical processes such as oxidation may modify this surface state. Also, the influence of a slight variation of the beam energy may become important. Even if the accelerating voltage is perfectly stabilized, a slowing down of the electrons may result from passing through a contamination layer, or from charge effects in the case of insulators.

It will therefore be prudent to maintain the rate of excitation between the limiting values 1.5 and 2; the discrimination is then close to its optimum value without the disadvantages noted being too troublesome.

3. *Possibility of Improving the Discrimination.* From the considerations

¹³ See Sec. III, D.

¹⁴ See Sec. III, E, 2.

which have just been set down it follows that the discrimination power of spot analysis can easily be brought to the neighborhood of $1\ \mu$, with a possibility of pushing the limit back to about $0.3\ \mu$ under the best conditions. The further lowering of this limit requires some considerable effort and it seems clear that the only possibility of an important advance in this line lies in the analysis "by transmission" of previously thinned down samples, as was suggested by the author (1, 42).

Suppose for instance that the sample to be analyzed is no longer in the form of a solid sample, but in the form of a thin film, the thickness of which is much less than the maximum range of the electrons. The deviation of the electrons in passing through the sample is then very slight and the diameter of the analyzed region is practically equal to the diameter of the probe. Discrimination is then limited only by current considerations, and this limitation is much less harsh than in the case of solid samples, since the accelerating voltage can be held at a sufficiently high value to ensure good efficiency of the electron-photon conversion. In the case of solid samples, improvement in the discrimination power can be obtained only at the cost of a catastrophic collapse of this efficiency. It will even be worthwhile to use relatively high voltages for the analysis of thin films, for the following reasons:

(1) The mean deviation of the electrons on crossing a layer of a given thickness falls as the initial energy of the electrons increases; this mean deviation depends only on the ratio of the energy of the electron to its initial energy (43) and tends to zero as this ratio tends towards unity.

(2) The ratio of the intensity of the line to that of the continuous spectrum recorded simultaneously in the spectrometer (signal-to-background ratio) increases with the electron accelerating voltage. If we consider the emission as a whole in all directions, we find that the intensity of the continuous spectrum over a band of wavelengths of a given width enclosing the line varies as V^{-1} (44a) while the intensity of the characteristic line varies roughly as $V^{-1}(V_K^{-1} - V^{-1})$ (44b); so that the line-background contrast increases with V and tends to a constant value for very high accelerating voltages. But, in addition, the direction of maximum emission of the continuous spectrum tends to move towards the beam direction at high energy (44c). As a result of this fact if the X-ray beam analyzed is on the side of the bombarded surface of the sample, it contains practically only the characteristic line as soon as the beam accelerating voltage becomes large (100 kv, for instance).

(3) The probe brightness is proportional to V for a given diameter, and this is quite an advantage since the main limitation in the discrimination power arises in this case from current considerations. The discrimination power can be estimated in the following way:

In the case of analysis by transmission of a thin layer, the X-ray emission is considerably reduced by the fact that the path of the electrons inside the sample is very short. Suppose for example that the measurement of line intensity is always effected by means of a curved quartz spectrometer and that the sample consists of a thin copper foil ϵ microns thick ($\epsilon \ll 1$). From the measurements made by Castaing and Descamps,¹⁵ it can be deduced that the ratio of the Cu $K\alpha_1$ emission of this layer to the Cu $K\alpha_1$ emission, under the same bombardment conditions, of a solid copper anti-cathode is

$$\frac{I_*(\text{Cu})}{I(\text{Cu})} = \frac{\rho\epsilon}{14.6} \approx 0.6\epsilon, \quad (32)$$

for an accelerating voltage of about 30 kv. Let us measure the intensities of the characteristic radiations in pulses per second in the counter. If i is the beam current in microamperes, we have

$$I(\text{Cu}) = 60,000i, \quad \text{or} \quad I_*(\text{Cu}) = 36,000i\epsilon. \quad (33)$$

If the examination of the sample is performed by transmission electron microscopy, a reducing lens of very short focal length can be used; we are therefore under "ideal probe conditions" ($V = 30$ kv) and we obtain from Eq. (18)

$$I_*(\text{Cu}) = 5.77 \cdot 10^6 \epsilon d^{8/3}, \quad (34)$$

where d is the diameter of the probe in microns. For a sample 0.2μ thick and a probe diameter of 0.1μ , the Cu $K\alpha_1$ intensity is 250 counts/sec, the discriminating power being close to 0.1μ ; such an intensity is quite sufficient for a correct measurement of characteristic emission.

However, it will be noted that the intensity of the characteristic lines decreases more or less as the $11/3$ power of the resolution, and there is not much hope of improving the latter with the same experimental arrangement. There are then two possibilities:

- (1) Increasing the probe brightness by correcting the spherical aberration or using a field emission gun.
- (2) Replacing the spectrometer by a nondispersive system securing high collection efficiency; the solid angle of the beam received by the curved quartz spectrometer is about $1/300$ steradian and so it can be hoped to attain, in the limit, a gain of about five in the discrimination power.

The ultimate discrimination of transmission microanalysis would then be in the neighborhood of 0.02μ ; we have seen that thermal limitations do not play any part (at least in the case of metal films).

¹⁵ See Sec. III, B.

On the other hand, the contamination of the sample, which is a function of the total beam current, will be fairly rapid, and it can be expected from practical considerations of available space around the specimen that it will be even more difficult to eliminate it completely than in the case of solid samples. It might be feared that the contamination layer might cause a serious perturbation; in actual fact this cause of error is not at all serious in the case of transmission analysis. The main effect of crossing a contamination layer is to slow down slightly the incident electrons. This slowing down would cause a large variation of the characteristic emission in the case of a solid sample bombarded by electrons with an energy close to the critical excitation energy of the X level; but it has no appreciable effect on the emission of a thin layer bombarded by high-energy electrons. This behavior can be observed on the experimental curves (variation of the ionization function with the rate of excitation V/V_K) obtained by Webster, Hansen, and Duveneck (44d). The only effect of the contamination layer, therefore, is to introduce some diffusion of the electrons which slightly lowers the discrimination. From Bothe's formula, the most probable angular deviation suffered by 50-kv electrons after passing through a contamination layer (mainly carbon) 0.1μ thick would be about 3° . The loss of discrimination is negligible, and the same applies to the lengthening of the electron trajectories within the thin sample. The latter point is an important one since the result of the analysis is not to supply directly the concentrations of the element present at the point analyzed, as is the case for solid samples, but the masses per unit area of these various elements. It is therefore necessary to measure in turn all the elements present in order to obtain the chemical composition of the sample. A gradual inclination of the electron trajectories within the sample could thus lead, if the various elements are measured in turn, to a slight overestimate of the elements measured last, when the contamination layer becomes rather thick. In actual fact, the effect is a second order one, and the same applies to the error introduced by the formation of a superficial film of any kind (oxidation, for instance) provided of course that it is not the element to be measured which gets deposited on the sample.

Analysis by transmission measures directly the superficial masses of the various elements present at the analyzed point. Any surface phenomenon such as oxidation or deposition of a contamination layer which leaves these superficial masses unvaried (it is assumed that the element measured is neither oxygen nor carbon!) has no effect on the results of the measurements.

4. *Experimental Verifications.* Many processes can be used for estimating approximately the diameter of the X-ray source constituted by the analyzed region. For example, this source can be used to form the image

of a very fine grid by X-ray shadow microscopy. It is also possible to estimate visually the resolution on the image obtained by X-ray scanning microscopy (37). For an accurate measurement of the true discrimination power (i.e., of the minimum diameter of the region where an accurate quantitative analysis is possible), the best method consists of analyzing a specimen showing abrupt phase boundaries such as a diffusion couple or better a composite sample obtained by pressing two metals against one another. As an example, one can verify, by scanning the probe across a copper-tantalum boundary, that a movement of $1.2\ \mu$ of the probe is sufficient to raise the Cu $K\alpha_1$ emission from 0 to 100% (after correction for the secondary fluorescence emission) when the accelerating voltage is 14 kv, while the minimum displacement is $3\ \mu$ for an accelerating voltage of 30 kv. In the analysis of thin samples, one may mention the discrimination of $0.3\ \mu$ obtained by Duncumb with an accelerating voltage of 25 kv (41).

It should be noted that, in what has already been said, absolute discrimination is referred to, i.e. the total diameter of the region excited by the electron beam. Resolution could also be defined in a manner similar to that used in optics, by means of samples with a periodic structure formed by stacking alternate layers of element A and element B. A movement of the probe through the sample then reveals its periodicity, even if the latter is much smaller than the absolute discrimination. The resolution of an image obtained in X-ray scanning microscopy can therefore be, provided the differences of chemical composition are sufficiently marked from one point to the next one, considerably greater than the absolute discrimination of the same instrument for precision quantitative analysis.

In regard to the detection of small particles (analogous to ultramicroscopy in the case of light), the limit is even lower; iron inclusions less than $0.1\ \mu$ in diameter can be detected in a sample of medium atomic number.

III. THE FUNDAMENTALS OF QUANTITATIVE ANALYSIS BY X-RAY EMISSION

We have seen in Sec. I that the concentration of an element A in a complex sample is measured by comparing the intensity I_A emitted by the sample in a strong characteristic line (A $K\alpha_1$ for example) of element A with the intensity $I(A)$ emitted in the same line and under the same bombardment conditions by the pure element A. The intensities I_A and $I(A)$ are the intensities actually emitted by the atoms of the anticathode directly ionized by the electron beam. In order to obtain them it is important to apply various corrections to the raw intensities read in the spectrometer (apart from the correction for dead time of the counter).

A first correction consists in subtracting from each reading the part due

to the portion of the continuous spectrum recorded simultaneously by the spectrometer; this correction is readily obtained by taking the mean of the intensities recorded for two settings of the spectrometer on either side of the line; it is generally small as long as the concentration of the element being measured is greater than a few per cent.

It is then necessary to subtract from the intensity obtained the fraction of that intensity arising from an excitation of the sample by the X-rays themselves (characteristic radiation and continuous spectrum); it is this correction for fluorescence which proves to be the most difficult to evaluate with accuracy.

Finally, the intensity of the line must be corrected for its absorption in the anticathode itself [the other absorptions in the outlet window, in air, etc. do not enter since they are eliminated when taking the ratio $I_A/I(A)$]. This absorption correction may become particularly large in certain extreme cases, and it is essential to apply it very carefully.

A. Absorption Correction

To take an example, let us consider a plane anticathode consisting of the pure element A, of density ρ , receiving normally on its surface an electron beam with an accelerating voltage V , and let us designate by θ the angle of emergence of the X-ray beam analyzed. Let I be the intensity which would be recorded by the spectrometer if there were no X-ray absorption in the anticathode, and let dI be the fraction of this intensity which is emitted by an infinitely thin layer with a thickness dz located at a depth z under the surface of the anticathode. Measuring the thicknesses in masses per unit area, we shall write

$$dI = \varphi_A(\rho z) d(\rho z). \quad (35)$$

The function φ_A , which we shall reconsider later, represents the distribution in depth of the characteristic emission $A K\alpha_1$ in an anticathode formed of the element A and subjected to normal electron bombardment with an accelerating voltage V .

In the absence of X-ray absorption in the anticathode, the spectrometer would then record an intensity

$$I = \int_0^\infty \varphi_A(\rho z) d(\rho z). \quad (36)$$

In actual fact, since the mass absorption coefficient of the radiation $A K\alpha_1$ in the anticathode is μ/ρ , the spectrometer records an actual intensity I'

$$I' = \int_0^\infty \varphi_A(\rho z) \exp\left(-\frac{\mu}{\rho} \rho z \operatorname{cosec} \theta\right) d(\rho z); \quad (37)$$

from which we shall obtain the intensity corrected for absorption by the relation

$$I = I' \frac{F(0)}{F\left(\frac{\mu}{\rho} \operatorname{cosec} \theta\right)}, \quad (38)$$

where F is the Laplace transform for the function φ_A

$$F(\chi) = \int_0^\infty \varphi_A(u) \exp(-\chi u) du. \quad (39)$$

The curve which represents the variation of the function $F(\chi)/F(0)$ as a function of the argument $\chi = (\mu/\rho) \operatorname{cosec} \theta$ has been obtained directly by the author (2) in the case of an iron anticathode, by a method which consisted of examining the variation of the characteristic emission as a function of the angle of emergence θ ; it was used as a single absorption correction curve which was supposed to be valid, provided the electron accelerating voltage remained always the same, for all samples and all characteristic radiations, at least in a first approximation. This amounts to assuming that the function φ depends broadly only on the beam accelerating voltage, and constitutes a somewhat rough approximation. In actual fact, an exact determination of absorption correction requires a knowledge of the law of distribution in depth of the X-ray emission in the anticathode. We shall give a brief description of the experiments which have enabled Castaing and Descamps (7, 45) to determine directly the form of the function φ for various types of anticathodes.

B. Distribution in Depth of the Characteristic Emission

1. *Experimental Determination of the Distribution.* In order to determine experimentally the variation of the function $\varphi(\rho z)$, it is necessary to isolate the emission of a thin slice of the anticathode with a constant thickness dz , located at varying depths below the surface. The intensity read on the spectrometer represents, of course, the total characteristic emission of the slice dz multiplied by some coefficient. This coefficient, which depends on the aperture of the X-ray beam analyzed, on the efficiency of the spectrometer, on the absorption by the windows, etc., is invariable, provided the spectrometer setting and the characteristics of the electron beam are unchanged during the whole of the series of measurements and provided also that the result of the measurement is each time corrected for absorption in the anticathode itself; this absorption depending on the depth of the emitting layer.

It is then possible to refer the intensities emitted by the layer dz at the various depths to a common unit. This unit is the intensity of the characteristic radiation emitted under the same conditions by an identical layer

dz isolated in space and subjected to the same normal electron bombardment conditions. The unit so chosen is directly related to the value of the ionization function and to the thickness of the layer dz . Because the layer is infinitely thin and the beam normal to the surface, the path length for each electron is exactly equal to dz . The choice of this unit therefore enables the function $\varphi(\rho z)$ to be obtained in absolute terms.

In order to separate from the total emission of the anticathode that of a particular layer, Castaing and Descamps use an artifice which consists in replacing, in the massive anticathode consisting of the element A, the layer dz by a thin layer of an element B close to element A and whose properties are substantially the same as regards diffusion and deceleration of the electrons. Layer B then acts as a "tracer" whose characteristic $B K\alpha_1$ emission

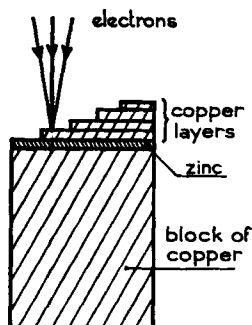


Fig. 16. Tracer composite sample for determining φ_{Cu} (Castaing and Descamps).

(say) can be easily separated by the spectrometer from the $A K\alpha_1$ emission of the anticathode as a whole. The choice of the tracer is limited by the following considerations: The element of which it is composed must be as close as possible in the periodic table to element A which makes up the anticathode; its characteristic emission must not be liable to secondary excitation by an intense line of element A, and the line emitted by the tracer must be only slightly absorbed by element A, so as to reduce the correction for absorption in the anticathode.

Suppose we have to determine the law of distribution $\varphi_{Cu}(\rho z)$ of the characteristic emission in an anticathode of pure copper. A carefully polished block of copper is covered, by vacuum deposition, with a zinc layer approximately 0.03 mg/cm^2 thick. An identical zinc layer is collected on a thin collodion film placed in the evaporator in the immediate neighborhood of the surface of the copper block. This layer can later be considered as isolated, the collodion playing an entirely negligible part. Then, on various regions of the surface of the block already coated with zinc, copper layers are deposited (Fig. 16) with increasing thicknesses, such as for instance 0.05 ,

0.1, 0.2, 0.5, 1, and 2 mg/cm². The various layers are deposited simultaneously on large plates, which makes it possible to determine their thickness accurately by weighing, at the cost of a few corrections. This procedure provides the whole of the experimental equipment required, i.e. zinc layers of rigorously equal thickness, one being isolated and the others more or less deeply buried in a copper anticathode. Then, by means of the spectrometer, a measurement is made of the intensity emitted in the Zn $K\alpha_1$ line when the various parts of the surface, which correspond to various values of depth z , are successively brought under the impact of an electron probe with constant accelerating voltage and current. For the common unit, the intensity is taken which is recorded in the spectrometer when the probe strikes the zinc layer deposited on the collodion. This series of measurements gives the curve of variation of the function $\varphi_{Cu}(\rho z)$. There is no need to take into account the radiation absorption in the zinc layer since the correction term is eliminated when taking the ratio of the two intensities, but, each intensity measurement is corrected for the absorption suffered by the Zn $K\alpha_1$ radiation in the superficial copper layer. Also, it is necessary to take into account the fact that the zinc layer has a finite thickness. This is done by sliding the curve in a direction parallel to the ρz -axis by an amount equal to half the superficial mass of this layer.

2. *Interpretation of the Results.* Figure 17 shows the curves of distribution in depth of the characteristic emission in copper (zinc tracer), aluminum (copper tracer), and gold (bismuth tracer) obtained by Castaing and Descamps for a beam accelerating voltage of 29 kv.¹⁶ The abscissas represent the depth in mg/cm², while the ordinates show $\log \varphi$. It will be noted that the unit, i.e. ordinate 0, corresponds to the emission of the tracer isolated in space and subjected to bombardment by the same electron beam. These curves suggest the following remarks:

(1) The value of φ for zero depth is always greater than unity, the tracer emission being reinforced by the underlying block. This effect is mainly due to back-scattering of the electrons. A slight increase also arises from the excitation of the tracer by the continuous spectrum of the anticathode as a whole. But it can be verified that it is important only in the case of heavy elements (compare Figs. 17 and 18). Back-scattering increases with the value of the atomic number of the anticathode; after correction for fluorescence (Fig. 18) we obtain

$$\varphi_{Al}(0) = 1.16; \varphi_{Cu}(0) = 1.475; \varphi_{Au}(0) = 1.613.$$

(2) The function φ starts to increase for small depths; this is due to the gradual diffusion of the electrons which lengthens their path within the dz layer (2). The effect of this gradual diffusion is felt down to a depth cor-

¹⁶ Further measurements have slightly lowered the tail of the gold curve.

responding to a condition of complete diffusion, from which point the mean angle of incidence of the electrons on the tracer becomes constant.

(3) When the complete diffusion is established, φ decreases proportionately to the number of electrons reaching the layer, as shown by Fig. 18 where the t_{Cu} curve represents the absorption curve of electrons in copper (7). This proportionality is due to the fact that, in these measurements, the beam accelerating voltage is much higher than the critical excitation voltage of the X-ray levels. This linear behavior would not appear in the case of

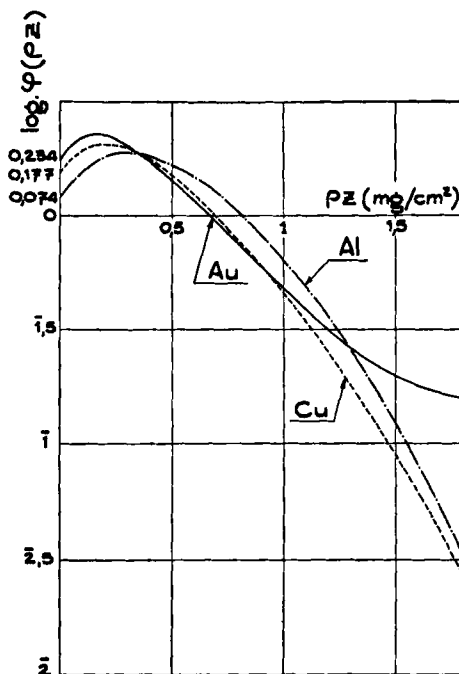


FIG. 17. Distribution in depth of the total emissions (Castaing and Descamps).

low accelerating voltages leading to optimum discrimination. For instance, in the determination of φ_{Al} , the replacement of the copper tracer by a bismuth tracer for which the rate of excitation is much lower (7) leads to a faster decrease of φ_{Al} for the deeper layers.

The depth z_d where complete electron diffusion is established increases when the atomic number of the diffusing element decreases. For aluminum, complete diffusion is reached only at a depth corresponding to $\rho z_d = 0.6$ mg/cm², it is already reached in the case of copper for $\rho z_d = 0.4$ mg/cm², and in gold for $\rho z_d = 0.25$ mg/cm² (Fig. 18).

(4) For the deeper layers, the decrease of φ (total characteristic emis-

sion of the tracer, Fig. 17) is slower, this effect being particularly marked in the case of gold. This behavior is due to the fluorescence secondary emission of the tracer, excited by the general continuous spectrum of the anticathode. It will be seen a little further on¹⁷ how this fluorescence emission can be estimated approximately. By deducting it from the experimental values shown in Fig. 17, the curves of Fig. 18 are obtained; these represent

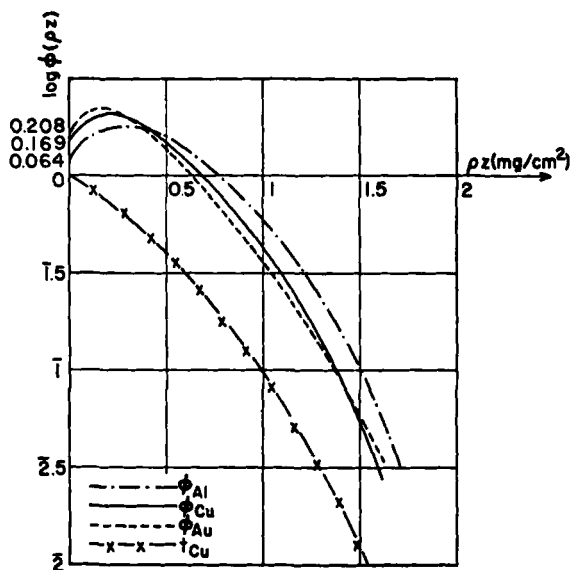


FIG. 18. Distribution in depth of the direct (primary) emissions and absorption curve of electrons in copper (t_{Cu}) (Castaing and Descamps).

the distribution in depth of the direct characteristic emission (i.e. directly excited by the electron beam) of anticathodes of aluminum, copper, and gold for an accelerating voltage of 29 kv. This deduction is based on the assumption that the fluorescence emission of the tracer is approximately the same at all depths till 1.5 mg/cm². It is then found that the constant contribution of fluorescence emission is: for aluminum, $\varphi_{Al}^f = 0.025$ (selective absorption of the continuous spectrum in the copper tracer), for copper, $\varphi_{Cu}^f = 0.03$, and for gold, $\varphi_{Au}^f = 0.10$.

C. The Physical Basis of the Emission-Concentration Relation

The distribution curves of Fig. 18 enable us to analyze in greater detail the various factors entering in the relation connecting the characteristic emission of the various elements of a complex anticathode with their respective concentrations.

¹⁷ See Sec. III, E, 2.

Consider an anticathode formed of an alloy AB in which the mass concentrations of elements A and B are respectively c_A and c_B . Let φ_A and φ_{AB} be the respective distribution functions of the radiation A $K\alpha_1$ in the pure element A and in the alloy AB. As before, we shall designate I_A and $I(A)$ as the intensities emitted in the A $K\alpha_1$ line, under the same conditions of electron bombardment, by the alloy AB and by the pure element A. As regards the X-ray emission, the anticathode AB behaves as if it consisted of a stack of infinitely thin layers of elements A and B. This gives immediately

$$\frac{I_A}{I(A)} = c_A \frac{\int_0^\infty \varphi_{AB}(\rho z) d(\rho z)}{\int_0^\infty \varphi_A(\rho z) d(\rho z)} = c_A \frac{S_{AB}}{S_A} \quad (40)$$

where S is the integral from zero to infinity of the function φ . Consider the special case for which c_A is infinitely small, φ_{AB} is then the same as the function φ_B which represents the distribution of the characteristic emission B $K\alpha_1$ obtained by means of an A tracer, and we can write

$$\frac{I_A}{I(A)} = c_A \frac{S_B}{S_A}. \quad (41)$$

It therefore appears that the approximate emission-concentration proportionality $I_A/I(A) = c_A$ is nothing else than an approximate equality of the integrals S_A and S_B and is obtained in this case with the same relative error. We shall therefore obtain an idea of its degree of accuracy by comparing the S integrals of the various elements.

Referring to the distribution curves of Fig. 18 (direct emissions), we find the following numerical values

$$S_{Al} = 1.55 \times 10^{-3}, S_{Cu} = 1.46 \times 10^{-3}, S_{Au} = 1.43 \times 10^{-3}.$$

The unit is the intensity which would be emitted under the same conditions by a layer of the same element of mass per unit area 1 gm/cm², normally crossed through by the electron beam, if the electrons of this beam were to retain their energy throughout the path and if there were neither electron diffusion nor fluorescence emission.

These values are close to one another; the agreement between S_{Al} and S_{Cu} would even be improved by using the same tracer for the two distribution curves, as is supposed in deriving Eq. (41). Considering the φ_{Al} curve obtained by Castaing and Descamps (?) with a zinc tracer and correcting it for fluorescence, we obtain $S_{Al} = 1.45 \times 10^{-3}$; we may conclude that the integrals are found to be equal to within the accuracy of determining $\varphi(\rho z)$ —about 2%.

An exact determination of the φ curves would make it possible, by com-

paring curves obtained with the same tracer, to calculate the α_i coefficients of the second approximation [Eq. (11)]. However, a direct determination of the α_i coefficients by the analysis of alloys of known composition is much simpler and more precise than the experimental plotting of the distribution curves. The relation $\alpha_A/\alpha_B = S_B/S_A$ (same tracer) is really only of theoretical interest, but it shows that the variation of the α coefficients from one element to another is slower than that of the Z/A ratios which appear in the theoretical second approximation deduced from Webster's law of deceleration [Eq. (8)]. This discrepancy is due to back-scattering which acts inversely to the factor Z/A in Webster's equation.

As a result of back-scattering, many beam electrons leave the anticathode with an energy definitely greater than the critical excitation energy of the line analyzed. The intensity $I(A)$ emitted by an anticathode of pure element A is thus less than the intensity $I_0(A)$ which the anticathode would emit if there were no back-scattering and if, in consequence, the whole of the electron trajectories were located within the anticathode. Let us define this "back-scattering loss" by introducing the coefficient $\lambda_A = I_0(A)/I(A)$; the back-scattering loss is then $(\lambda_A - 1) I(A)$ and the coefficient λ_A , always greater than unity, is greater the heavier the element. Applying then the theoretical second approximation [Eq. (8)] to the emissions corrected for back-scattering, we obtain the relation

$$\frac{\alpha_A}{\alpha_B} = \frac{\lambda_A (Z/A)_A}{\lambda_B (Z/A)_B}. \quad (42)$$

It thus appears that each α_i is the product of two factors, the first one of which increases with atomic number Z while the second decreases with increasing Z . This "compensation" is the reason why the values of α_i vary but little from one element to another.

It is possible to get a rough estimation of the values of the λ coefficients, (back-scattering correction) by an examination of the curves of distribution in depth of the characteristic radiation (Fig. 18). It can be taken roughly that the back-scattered electrons which reach the free surface have on the average followed the same path in the anticathode as those which reach the layer at depth $z_1 = 2z_d$ (z_d being the depth from which the electron trajectories are completely diffuse). For each anticathode it will be assumed that the back-scattering loss is approximately equal to the total emission of the anticathode layers situated below the depth z_1 , or

$$I_0(A) - I(A) = \int_{z_1}^{\infty} \varphi_A(\rho z) d(\rho z), \quad (43)$$

and hence

$$\lambda_A = 1 + \frac{\int_{z_1}^{\infty} \varphi_A(\rho z) d(\rho z)}{\int_0^{\infty} \varphi_A(\rho z) d(\rho z)}. \quad (44)$$

This gives:

$$\begin{aligned} \text{For copper} \quad (Z/A = 0.456): \rho z_1 &= 0.8 \text{ mg/cm}^2; \lambda_{\text{Cu}} = 1.15; \\ \text{For aluminum} \quad (Z/A = 0.482): \rho z_1 &= 1.2 \text{ mg/cm}^2; \lambda_{\text{Al}} = 1.05; \\ \text{For gold} \quad (Z/A = 0.400): \rho z_1 &= 0.5 \text{ mg/cm}^2; \lambda_{\text{Au}} = 1.34. \end{aligned}$$

If we arbitrarily make $\alpha_{\text{Cu}} = 1.00$, we find from Eq. (42) the α_i coefficients

$$\alpha_{\text{Al}} = 0.96, \alpha_{\text{Cu}} = 1.00, \alpha_{\text{Au}} = 1.02,$$

in excellent agreement with the values which might be deduced from consideration of the S integrals.

The method which has been followed for the estimation of the back-scattering loss can be supported by the following remarks:

(1) The curve of electron absorption in copper (Fig. 18) shows a transmission factor of about 20% for 29-kv electrons passing through a copper layer of 0.8 mg/cm². This value is not very different from the percentage of back-scattered electrons, i.e. 29%.

(2) It will be noted that in each case the following relation is approximately verified:

$$\varphi_A(\rho z_1) = 2[\varphi_A(0) - 1]. \quad (45)$$

But, the bracket in the second term represents the fraction of the emission of the superficial layer due to the back-scattered electrons as this superficial layer is crossed (from bottom to top) by the back-scattered electrons. The number of these electrons is about the same as the number of electrons which pass downward through the layer at depth z_1 . The factor 2 can be interpreted if it is assumed that, because of the completely diffuse distribution of the trajectories, the layer z_1 is crossed by an equivalent number of electrons traveling upward.

(3) If the φ_{Cu} curve is compared with the t_{Cu} curve representing electron transmission in copper for the same accelerating voltage (Fig. 18), it will be seen that, at medium depths for which complete diffusion is attained without too severe a loss of energy by the electrons, the relation

$$\varphi_{\text{Cu}} = 4t_{\text{Cu}} \quad (46)$$

is substantially verified, t_{Cu} being the electron transmission factor. This relation means that the mean path length, in the dz layer, of the electrons which have passed through a thickness large enough for complete diffusion is of the order of 4 dz . If we assume, as before, that each of these electrons passes, on the average, twice through the dz layer, we obtain, calling θ the angle of incidence of the electron trajectory on the dz layer:

$$|\sec \theta| = 2 \quad (47)$$

which is exactly the value which can be expected from a completely random distribution of the trajectory directions (cosine distribution).

D. Experimental Absorption Correction Curves

From the experimental curve of distribution in depth of the characteristic emission of a given element A (for a given accelerating voltage V), it is easy to plot the Laplace transform $F(\chi)$ [Eq. (39)]. The curve which represents the quantity $\log [F(\chi)/F(0)]$ as a function of the argument $\chi = (\mu/\rho) \text{ cosec } \theta$ constitutes the absorption correction curve. Figure 19 shows the

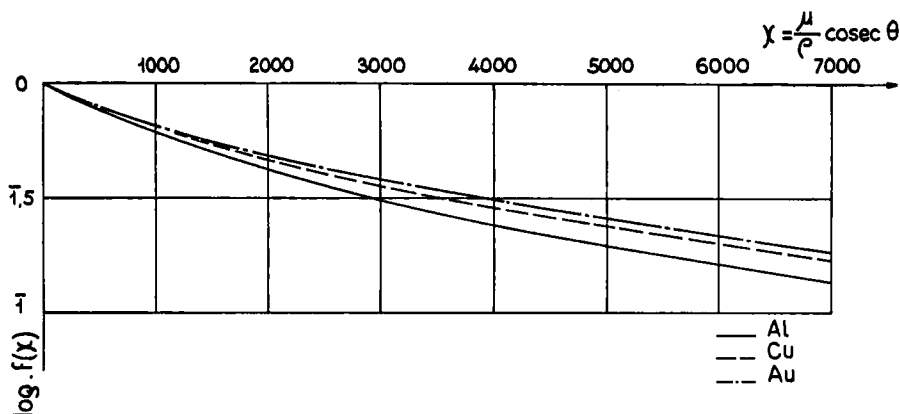


FIG. 19. Absorption correction curves (29 kv) (Castaing and Descamps).

absorption correction curves (direct emission) obtained in this way from the distribution curves of Fig. 18, for an accelerating voltage of 29 kv and anticathodes of aluminum, copper, and gold. The curve previously obtained by the direct method of variation of the X-ray intensity as a function of the angle of emergence (2) would lie satisfactorily in this family of curves (36). The various curves are much alike, but it will be noted that, for an accurate determination of absorption correction, it is necessary to take into account the average atomic number of the region analyzed.

Absorption correction can become quite large when analyzing light elements whose characteristic lines are easily absorbed. In this case values of χ of the order of 5,000 to 10,000 are commonly found. The use of an accelerating voltage of 30 kv for the beam would then involve an enormous absorption correction, more than 80% of the emitted intensity being absorbed within the sample. It is then necessary to use the lowest possible accelerating voltage in order to limit the absorption correction to 30 or 40%. It is important to ensure that this correction shall remain fairly small since one can never be sure of its rigorous accuracy. For however carefully the absorption curves have been prepared, there always remains some uncertainty in the value of θ since the angle of emergence may be locally

modified by an amount of the order of 1° . This is the case when analyzing a precipitate which is generally protruding or slightly recessed after mechanical polishing. In any case it is necessary to perform this polishing with care and to avoid electrolytic polishing, especially in the case of light alloys where it would be, in other respects, particularly convenient.

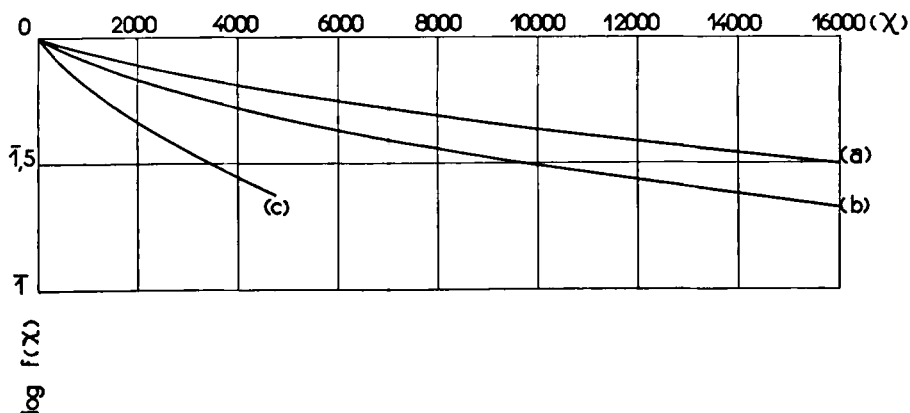


FIG. 20. Absorption correction curves for different voltages and average atomic numbers; (a), $V = 9.7$ kv, $\bar{Z} = 13$; (b), $V = 15.1$ kv, $\bar{Z} = 13$; (c), $V = 27.5$ kv, $\bar{Z} = 26$ (Castaing and Descamps).

Figure 20 shows the absorption correction curves corresponding to various accelerating voltages and various kinds of anticathodes obtained by the direct method of variation of the X-ray intensity as a function of the emergence angle.

E. Fluorescence Correction

Secondary emission caused by fluorescence is a particularly troublesome phenomenon in the exact interpretation of the results obtained from the electron probe microanalyzer.

First, the emission-concentration proportionality, which is the basis of this method of analysis, is no longer true, in general, for the secondary emission. It is clear for instance that an element which strongly absorbs the exciting radiation suffers a selective excitation within the complex anticathode and that, as a result, there is an intensification of its apparent concentration. This situation will be clear immediately if we remember that the emission-concentration proportionality in the case of primary emission is directly related to the fact that all the elements possess broadly the same mass absorption coefficient for the beam electrons.

Also, it should be noted that, although the primary emission excited by an electron probe is strictly restricted to the very small volume swept through by the electrons, such is not the case for the secondary fluorescence

radiation, which may have its source in the whole of the region irradiated by the X-rays issuing from the point of impact of the probe. For example, spot analysis by X-ray spectroscopy of a very small precipitate in an alloy necessarily consists in superposing two analyses:

- (1) X-ray emission analysis of the precipitate itself,
- (2) Fluorescence analysis of the precipitate with its surrounding region.

It is therefore important to determine the value of this secondary fluorescence emission in order to estimate the correction term to be introduced in the results of the measurements, or at least an order of magnitude of the resulting uncertainty in the measurement of the various concentrations.

1. Excitation by Characteristic Radiations. An important source of secondary emission may arise from the excitation of the element analyzed by the characteristic radiations of a heavier element whose concentration is large. For example, in the case of an iron-chromium alloy with 10% chromium, the secondary fluorescence emission of Cr $K\alpha_1$ line excited by the K lines of iron is equal to 24% of the Cr $K\alpha_1$ intensity due to direct ionization of the chromium by the beam electrons (direct emission). Very fortunately, the case of excitation by characteristic lines lends itself rather well to calculation, and it is possible to estimate the secondary emission with a sufficient degree of accuracy to remove completely the error which might result in the determination of concentrations. The calculations have been made by the author (2) and the correction formula obtained. Although the expression is a rather complicated one, it is convenient to use and leads to an accuracy which is quite sufficient for the needs of the analysis. It should be noted that Wittry (19) has taken up the author's calculations in a more elaborate form, using the curves of distribution in depth of the characteristic emission plotted by Castaing and Descamps (7) and thus obtained a more rigorous estimate of the fraction of the fluorescence radiation excited by the characteristic radiations directed outside the anticathode.

Matters become a little more complicated when an estimate has to be made of the importance of the fluorescence emission excited by the general continuous spectrum of the anticathode, and two methods will be briefly given which permit the experimental determination of this secondary emission.

2. Excitation by the Continuous Spectrum. Castaing and Descamps (7) use two separate methods for determining the secondary fluorescence emission excited by the continuous spectrum. In the first method, analogous to that previously used by Webster (46), the surface of the anticathode of element A is covered, by vacuum deposition, with a layer of aluminum of a thickness sufficient to stop the electron beam completely. The emission of the underlying anticathode is then entirely due to the fluorescence excited

by the continuous spectrum of aluminum. This continuous spectrum has practically the same distribution in wavelengths as that which would be produced by the same electron bombardment on an anticathode of element A (atomic number Z), the intensity of each radiation being modified in the ratio of $13/Z$. After a few minor corrections (in particular absorption correction for the fluorescence radiation in passing through the aluminum layer) the experimental value of the ratio I_f/I is obtained. This ratio represents the proportion of secondary emission due to the continuous spectrum directed inside the anticathode to the total characteristic radiation, at the exit from the anticathode at an emergence angle of 16° (value

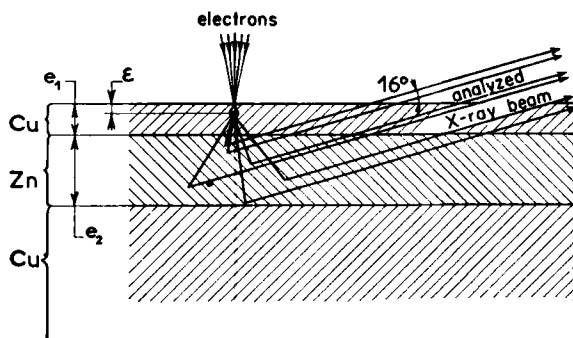


FIG. 21. Tracer composite sample for determining the true intensity of fluorescence emission excited by the continuous spectrum (Castaing and Descamps).

used by the authors). For example, the results obtained for an accelerating voltage of 29 kv are: for zinc, $I_f/I = 0.031$ and for bismuth $I_f/I = 0.059$. Further measurements have shown that this last value is probably a little low and that 0.07 would be a better figure.

The second method gives a direct determination of the relative value of the fluorescence emission, *as produced within the anticathode and before any absorption*. It uses the tracer process already used for the determination of the distribution in depth of the characteristic emission.

For example, suppose we wish to determine the magnitude of the secondary radiation in a zinc anticathode. A carefully polished block of copper is covered, by vacuum deposition, with a zinc layer of thickness e_2 and the whole is covered with a copper layer of thickness e_1 (Fig. 21). If the thickness e_1 of copper is sufficiently great to stop the electrons completely, then the Zn $K\alpha_1$ emission of the stratified layer is derived only from the excitation of the zinc layer by the continuous spectrum from the top copper layer. This continuous spectrum contains an infinite number of radiations occupying the whole of the frequency band between the quantum limit and the critical excitation frequency of the Zn K level. These various radiations

are very differently absorbed in the top copper layer and in the zinc layer, but it is possible, by a judicious choice of the e_1 and e_2 thicknesses, to arrange matters so that the fraction of the total intensity which is absorbed in the zinc layer is about the same for all the components of the exciting continuous spectrum (to within 10%). The experimental conditions are then as follows: A penetrating component of the continuous spectrum is weakly absorbed in the top copper layer and reaches the zinc at a high intensity; but only a small fraction of this intensity is absorbed in the zinc layer; a soft component is strongly absorbed in the top copper layer, its intensity is small when it reaches the zinc layer, but a large fraction of this intensity is absorbed by the latter. For a beam accelerating voltage of 20 kv, it is necessary to choose a thickness of zinc of the order of 4 mg/cm² (for absorbing a noticeable part of the continuous spectrum in it) and a thickness of copper of the order of 2 mg/cm². Under these conditions, the fraction of the continuous spectrum which is absorbed in the zinc substantially keeps the constant value of 0.32 from one end of the spectrum to the other.

After a few minor corrections, the authors obtain in this way the proportion I_f°/I of fluorescence emission due to the continuous spectrum, as produced within the anticathode and before any absorption; the value obtained for a zinc anticathode and a 20-kv voltage is $(I_f^\circ/I)_{\text{Zn}} = 0.068$.

If this is compared to the value obtained for the same voltage at the exit of the anticathode at an emergence angle of 16°, that is $(I_f/I)_{\text{Zn}} = 0.036$ (?), the large absorption suffered by the fluorescence radiation in the anticathode itself, because of its great mean depth of emission, is readily appreciated.

It would be easy to predict theoretically the ratio I_f/I_f° if the fluorescence emission were excited by a monochromatic radiation issuing from the surface of the anticathode. In this case we would have, designating respectively by μ and μ' the mass absorption coefficients in the anticathode of this exciting radiation and of the fluorescence radiation $\text{Zn } K\alpha_1$

$$\frac{I_f}{I_f^\circ} = \frac{\ln(1+x)}{x}, \quad \text{where } x = \frac{\mu' \operatorname{cosec} \theta}{\mu}. \quad (48)$$

Actually the exciting radiations occupy a band of wavelengths within which the quantity $\ln(1+x)/x$ varies from 0.37 to 0.82. It can be taken that the experimental ratio $I_f/I_f^\circ = 0.53$ represents the mean value of the quantity $\ln(1+x)/x$, averaged over the exciting spectrum taken as a whole.

This result enables us to obtain approximately the intensification by fluorescence due to the continuous spectrum in the case of a complex alloy. Since we are concerned only with an approximate calculation, we can replace the exciting spectrum by a single radiation emitted at the surface

of the anticathode. For example, suppose we have to determine the proportion of secondary emission due to continuous spectrum in the A $K\alpha_1$ line emitted by an alloy in which the mass concentration of A is c_A . Calling μ' the mass absorption coefficient of the A $K\alpha_1$ line in the alloy, $\bar{\mu}_{all}$ and $\bar{\mu}_A$ the mass absorption coefficients of the alloy and of the element A, for the mean exciting radiation, we obtain

$$\left(\frac{I_f}{I}\right)_{all} = \left(\frac{I_f}{I}\right)_A \frac{Z_{all}}{Z_A} \frac{\bar{\mu}_A}{\bar{\mu}_{all}} \frac{\ln(1+x)}{x}, \quad (49)$$

where

$$x = \frac{\mu' \operatorname{cosec} \theta}{\bar{\mu}_{all}}.$$

It may happen that the variations of the last three terms in the right-hand term of Eq. (49) compensate roughly for one another when varying c_A . Such is the case for aluminum-copper alloys where Cu $K\alpha_1$ is reinforced in about the same ratio at all concentrations, which in this particular case makes it unnecessary to apply the fluorescence correction.

The above calculations suppose that the sample is homogeneous over an extended region around the analyzed point. If we consider the opposite case where a very small precipitate is analyzed, imbedded in a matrix the chemical composition of which is quite different, we reach the conclusion (7) that:

(1) In the extreme case where the concentration of the analyzed element is zero in the matrix, neglecting the fluorescence excited by the continuous spectrum leads to a relative error in the concentration c_A in the precipitate

$$\frac{c'_A - c_A}{c_A} = - \left(\frac{I_f}{I}\right)_A, \quad (50)$$

c'_A being the apparent concentration.

(2) In the extreme case where the matrix consists entirely of the element which is being analyzed in the precipitate, neglecting the fluorescence leads to an absolute error of

$$c'_A - c_A = \left(\frac{Z}{Z_A} - c_A\right) \left(\frac{I_f}{I}\right)_A, \quad (51)$$

where Z_A is the atomic number of element A and Z the average atomic number of the precipitate. In this last case, the relative error can be enormous for small concentrations and it would be difficult to estimate it correctly. In such a case, determining c_A from measurements of the concentrations of the other elements present in the precipitate is highly recommended.

In conclusion Table I shows the various stages of the analysis of a gold-copper alloy by means of the Au $L\alpha_1$ line; the accelerating voltage used is 29 kv and the absorption correction is fairly large.

TABLE I. X-RAY EMISSION ANALYSIS OF COPPER-GOLD ALLOYS

1	2	3	4
True concentrations c_{Au}	$I_{Au}/I(Au)$ Rough values (total emerging intensi- ties)	$I_{Au}/I(Au)$ After fluorescence cor- rection (direct emis- sion emerging in- tensities)	$I_{Au}/I(Au)$ After absorption cor- rection (direct emission true in- tensities)
0.4035	0.356*	0.364	0.402
0.5393	0.484†	0.491	0.534

* Average value from 11 scanning analyses.

† Average value from 4 scanning analyses.

The true concentrations (chemical analysis) are shown in column 1. Column 2 gives the rough experimental values of the ratio $I_{Au}/I(Au)$, corrected for counter dead time and continuous spectrum background (the specimen surface was scanned under the probe to average out segregation effects). Column 3 shows the values corrected for fluorescence excited by the general continuous spectrum [Eq. (49)], and column 4 shows the final values after correction for absorption (Fig. 19). The emission-concentration proportionality is perfectly verified here, the agreement between column 1 and column 4 being as good as could be hoped for from the accuracy of measurements (about 0.5%).

F. Fixed-Time versus Fixed-Charge Measurements

It will be interesting to consider here the modification proposed by Wittry (19) which consists in referring the measurements of X-ray intensities not to a constant value of the number of electrons received by the sample (fixed-time measurement with constant beam intensity) but to a constant value of the number of electrons absorbed by the sample (fixed-charge measurement).

The fact that the proportion of back-scattered electrons is 29% for copper and 49% for gold (as was checked by the author under the same instrumental conditions) means that a value of the ratio α_{Au}/α_{Cu} of $51/71 = 0.72$ has to be introduced in order to interpret correctly the results of a fixed-charge analysis. Thus, the emission-concentration proportionality law, which is extremely practical for a first approximation so long as repeated measurements shall not have definitely established the values of the empiri-

cal α_i coefficients which should be applied to all elements, is deliberately dropped. This complication could be justifiable if it were proved that the hyperbolic law corresponding to the second approximation is better followed in the case of a fixed-charge measurement than in that of a fixed-time measurement; but such is not the case.

Wittry's argument is mainly based on the results obtained in the author's thesis (2) concerning the analysis of aluminum-copper alloys with various concentrations. Table II gives the true concentrations of these alloys (column 1) and the experimental values (column 2) of the ratio $I_{\text{Cu}}/I(\text{Cu})$ obtained for these alloys in fixed-time measurements (2). Column 3 shows the respective errors involved by the assumption that strict emission-concentration proportionality is valid in fixed-time measurements. From the values given in Column 2, it is possible to calculate the ratios $I'_{\text{Cu}}/I'(\text{Cu})$ which would have been obtained in fixed-charge measurements. Designating by r_{all} and r_{Cu} the respective back-scattering coefficients of the alloy and of the pure element copper, one obtains immediately

$$\frac{I'_{\text{Cu}}}{I'(\text{Cu})} = \frac{1 - r_{\text{Cu}}}{1 - r_{\text{all}}} \frac{I_{\text{Cu}}}{I(\text{Cu})}. \quad (52)$$

The best estimate for r_{all} should be

$$r_{\text{all}} = c_{\text{Cu}} r_{\text{Cu}} + c_{\text{Al}} r_{\text{Al}}. \quad (53)$$

Designating by α the ratio $c_{\text{Cu}}/\alpha_{\text{Al}}$ which has to be introduced for interpreting the fixed-charge measurements [$\alpha = (1 - r_{\text{Cu}})/(1 - r_{\text{Al}}) = 0.815$], one obtains from Eq. (53)

$$\frac{I'_{\text{Cu}}}{I'(\text{Cu})} = \frac{\alpha}{1 - (1 - \alpha)c_{\text{Cu}}} \frac{I_{\text{Cu}}}{I(\text{Cu})}. \quad (54)$$

Column 4 gives the values so obtained. Applying to these values the hyperbolic emission-concentration relation of the fixed-charge measurement ($\alpha_{\text{Cu}}/\alpha_{\text{Al}} = 0.815$) leads to the concentrations given in Column 5, which are practically identical to the concentrations obtained directly by assuming strict emission-concentration proportionality in the fixed-time measurement (Column 2). Since the percentage errors are practically the same (compare column 6 to column 3), it should be concluded that no improvement is brought about by fixed-charge measurements.

But, Wittry's calculations are based on the implicit assumption that the back-scattering coefficient r_{all} of the alloy is given by the relation

$$\frac{1}{1 - r_{\text{all}}} = \frac{c_{\text{Cu}}}{1 - r_{\text{Cu}}} + \frac{c_{\text{Al}}}{1 - r_{\text{Al}}} \quad (55)$$

TABLE II. FIXED-TIME VERSUS FIXED-CHARGE MEASUREMENTS (ALUMINUM-COPPER ALLOYS)

1	2	3	4	5	6	7	8	9
c_{Cu}	$I_{\text{Cu}}/I(\text{Cu})$ Fixed-time	Error (%) First approxi- mation, fixed- time $\alpha_{\text{Cu}}/\alpha_{\text{Al}} = 1$	$I'_{\text{Cu}}/I'(\text{Cu})$ Fixed-charge estimated from Eq. (54)	c_{Cu} From column 4 $\alpha_{\text{Cu}}/\alpha_{\text{Al}} =$ 0.815	Error (%) $\alpha_{\text{Cu}}/\alpha_{\text{Al}} =$ 0.815	$I''_{\text{Cu}}/I''(\text{Cu})$ Fixed-charge estimated from Eq. (56)	c_{Cu} From column 7 $\alpha_{\text{Cu}}/\alpha_{\text{Al}} =$ 0.815	Error (%) $\alpha_{\text{Cu}}/\alpha_{\text{Al}} =$ 0.815
0.01	0.0099	1	0.00808	0.0099	1	0.00808	0.0099	1
0.04	0.0373	6.75	0.0306	0.0373	6.75	0.0307*	0.0374	6.5
0.53	0.504	4.9	0.4555	0.506	4.5	0.460	0.5115	3.5
0.88	0.867	1.48	0.844	0.869	1.25	0.848	0.8725	0.85

* Witttry [Thesis, California Institute of Technology (1957)] obtains here the wrong figure 0.0317, leading to only 3.6% error in the concentration.

leading to the fixed-charge result

$$\frac{I''_{\text{Cu}}}{I'''(\text{Cu})} = [\alpha + (1 - \alpha)c_{\text{Cu}}] \frac{I_{\text{Cu}}}{I(\text{Cu})}. \quad (56)$$

Equation (55) seems to be less reliable than Eq. (53); but, even if one assumes its validity, consideration of Columns 7, 8, and 9 (Table II) makes it evident that the improvement brought about by the fixed-charge measurement is weak and vanishes at low concentrations.

Subtracting the fluorescence emission excited by the continuous spectrum would leave the results practically unaltered (the correction factor oscillates between 0.997 and 1.002).¹⁸

Moreover, recent measurements have shown that the large dispersion of the values $\alpha_{\text{Cu}}/\alpha_{\text{Al}}$ (fixed-time measurements) which appears to result from the author's experiments (2, 19) (Column 2 of Table II) is probably related to the extensive segregation which appears in these alloys and makes the results of the chemical analyses rather uncertain. New measurements will be necessary to clear up this last point.

As a conclusion, the complication involved in fixed-charge measurements is hardly justified by better results. Moreover, fixed-charge measurements depend directly on the electron current re-emitted by the sample, but, a not negligible fraction of this intensity is supplied by secondary electrons. This secondary emission is highly sensitive to the surface state of the sample and may suffer variations independent of the chemical composition of the underlying metal.

The author feels that until more data are available, it is more prudent to keep fixed-time measurement, in which the X-ray emissions of the sample and of the pure element are compared under identical conditions of electron bombardment.

IV. THE CONTRIBUTION OF MICROANALYSIS TO SCIENTIFIC RESEARCH

Electron probe microanalysis has been successfully applied to a lot of problems covering an extensive range of research fields; the most important of them is no doubt metallurgy. But stress must be laid on the fact that microanalysis can be carried out even on insulating materials, after coating them with a thin metal or carbon film by vacuum deposition for ensuring good electrical and thermal conductivities. This last possibility opens to the electron probe microanalyzer new fields of application such as mineralogy or even biology.

¹⁸ See Sec. III, E, 2.

A. Metallurgy

In the field of metallurgy, electron probe microanalysis has been used extensively for theoretical as well as technological studies. We will limit ourselves to a few examples picked up from the numerous papers which have already been published on this subject.

1. *Identification of Phases.* One of the important possibilities of this method is the identification of complex phases which appear as small precipitates, whose size lies generally between 0.1 and 10 μ . An example is given by the grey ternary phase appearing in the Al-Cu 6%-Fe 2% alloy. Various formulas had been proposed by different authors; spot analysis has shown (25, 47) that copper and iron concentrations (respectively $34.8 \pm 0.8\%$ and $14.2 \pm 0.6\%$) were consistent with the composition $\text{Al}_7\text{Cu}_2\text{Fe}$.

More difficult was an extensive study of zinc-rich complex brasses where the aluminum content was to be determined in very small two-phased starlike precipitates (48).

Nonmetallic inclusions, such as silicates, sulfides, phosphides, etc., which are generally present in steel are subject to identification only by quantitative determination of their medium atomic number components (Si, P, S, . . .) (49). An accurate quantitative analysis of the metallic elements makes it possible to distinguish between various types of carbides (M_3C , M_{23}C_6 , M_7C_3 , for instance) (50).

New methods of extracting replicas have enabled some workers to identify with the microanalyzer very small precipitates (size $< 1 \mu$) which were present in fracture surfaces of steel (51). Some siderurgical processes of steel production were not fully understood. By picking up the globular particles with diffuse boundaries which appear at the beginning of the temperature-steady state (1490°C) during the Thomas conversion of steel and analyzing the phosphorus content of these particles, it was possible to show that the particles were solid in the molten bath (52) (Fig. 22).

2. *Segregation.* Spot analysis has provided a most valuable tool in the study of various types of segregation which are not revealed by conventional metallographic methods. Researches in this field are quite numerous, mainly concerning technical problems (53-55). As an example, a map showing the segregation of manganese in Hadfield steel (C: 1.88%, Mn: 12.5%) has been obtained (Fig. 23) by plotting numerous point-by-point determinations (56). Curves of equal manganese concentration, different from one another by 0.5% Mn are drawn. This is a good example of what can be done automatically (57) by means of a scanning technique; although it should be noted that obtaining the same accuracy would require approximately the same bombardment time as point by point determination.

3. *Superficial Layers.* The best way of studying superficial layers con-

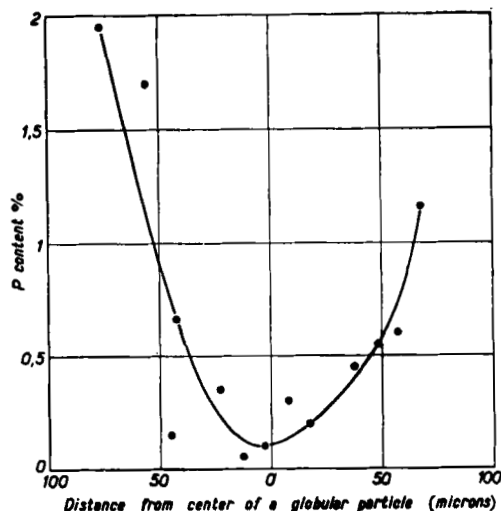


FIG. 22. Distribution of phosphorus across a globular particle (Thomas conversion of steel) (by courtesy of J. Philibert and Mrs. H. Bizouard) (52).

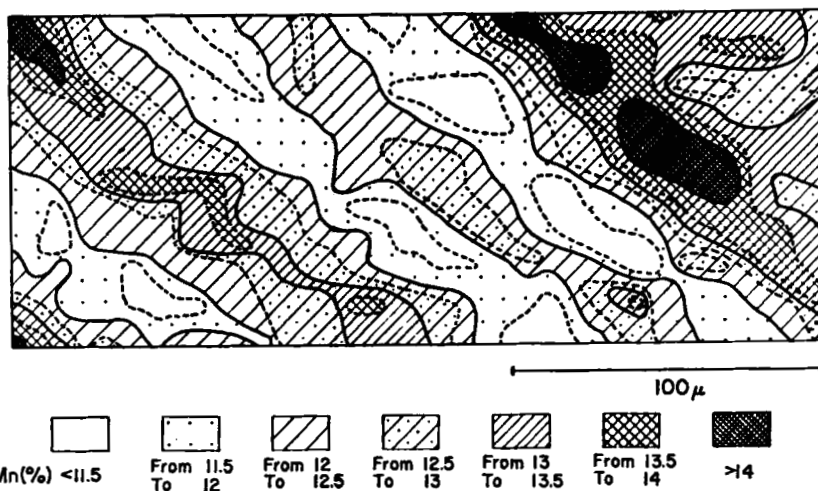


FIG. 23. Map showing segregation of manganese in Hadfield steel (by courtesy of J. Philibert and Mrs. H. Bizouard) (52).

sists in operating on a polished section of the sample previously imbedded in copper or any convenient metal by plating. If waxes or plastics are used, care must be taken to eliminate charging up effects and coating with a conducting layer is highly recommended. In any case, a polishing technique must be used which results in a flat surface, for level differences

at interfaces may introduce serious errors (absorption correction needs an exact knowledge of surface orientation).

Many kinds of layers have been investigated already, including corrosion layers as well as plating or chemical deposits. As an example, it was possible to show that in the new process of "sulfination," used to improve

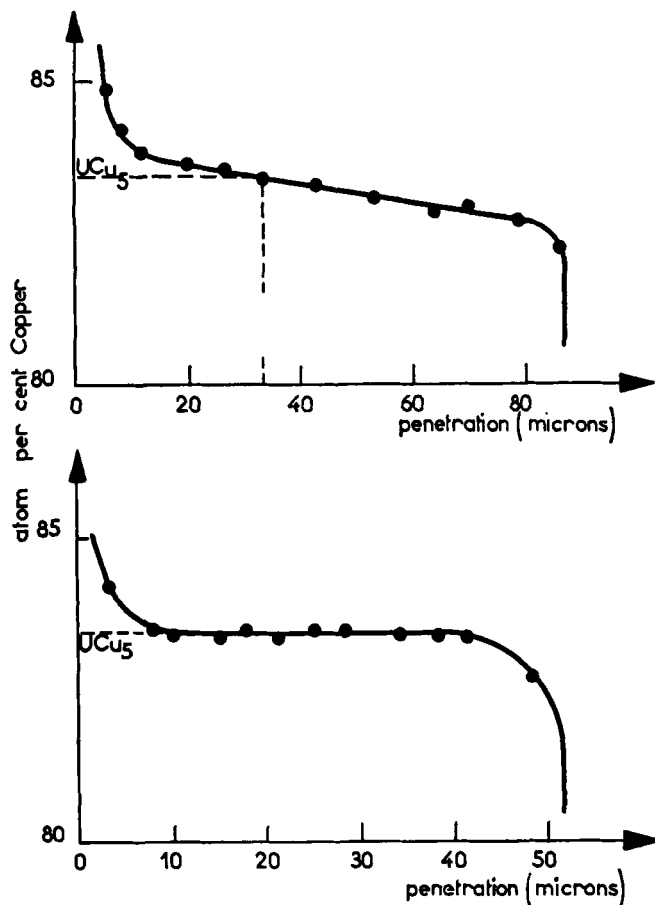


FIG. 24. Copper-uranium diffusion. Lower curve, under external pressure; upper curve, without external pressure (by courtesy of Y. Adda, M. Beyeler, and A. Kirianenko).

by a large amount the friction properties of mild steel, sulfur remains in the top thick superficial layer where it is located quite heterogeneously (58).

4. *Diffusion.* Drawing intermetallic diffusion curves was previously quite tedious work involving the preparation of a lot of samples; electron probe microanalysis needs only one sample and gives quickly and accurately

the whole diffusion curve without any preliminary calibration. An advantage of using this technique is that a special curve is obtained for each component (2). The method has been widely applied for determining diffusion constants, for studying the effect of ordering processes on the magnitude of mutual diffusion, for studying peculiarities in diffusion processes during the formation of substructure in single crystals and transfer processes between solid and liquid media (59).

Recently, a lot of work has been done on the diffusion of refractory metals such as titanium, molybdenum, and zirconium in uranium; the laws of diffusion have to be known quite well for the purpose of building nuclear reactors (60); variations of the diffusion coefficient and of the heat of activation have been determined, in the γ body-centered solution, directly from the diffusion curves obtained by spot analysis.

More precise equilibrium diagrams can be drawn from accurate measurements of the concentrations close to the interfaces of neighboring phases (55, 61).

Quite recently, accurate spot analyses have made evident an important phenomenon: the influence of external pressure on stoichiometric deviations in the intermetallic compounds prepared by diffusion. Heating a copper-uranium diffusion couple to 700°C for 48 hr gives rise to the upper diffusion curve shown in Fig. 24; the atomic concentration of copper is changed by 3% when going through the diffusion zone, which corresponds to a continuous change from $\text{UCu}_{4.7}$ (uranium side) to $\text{UCu}_{5.25}$ (copper side). The concentration gradient disappears when the diffusion couple is prepared under an external pressure of 500 kg/cm²; the concentration is then perfectly constant throughout the diffusion zone and corresponds to the UCu_5 stoichiometric composition (Fig. 24, lower curve) (62).

B. Mineralogy

In two main branches of mineralogy and petrography, electron probe microanalysis has already enabled workers to elucidate special questions concerning origin, development, and evolution of ore deposits. The first of these is the analysis *in situ* of ores and minerals in polished samples of stones coming directly from the pit or the sounding. We may cite here the extensive study of a complex copper-iron sulfide containing arsenic and tin; limits of concentration for the rather rare "orange bornite" have been given (25). Spot analysis has been applied to samples of polyphased ores containing elements whose determination by conventional methods would have been very difficult or even impossible. Maps of germanium and gadolinium concentrations have been drawn on polished sections of Tsumeb (Rhodesia) copper ore. It was also possible to determine the scandium and ytterbium content in Thortveitite (complex silicate), and to distinguish between

microinclusions (10–20 μ) of Xerotime (yttrium phosphate) and Zircon (zirconium and hafnium silicate) by measuring separately Y, Zr, and Hf (63).

A study of the French oolitic iron ore known as *minette lorraine* was taken into account in the planning of a new process of enriching the ore before melting in the high furnace (64).

The second area covers the analysis of dusts of various origins (volcanic, cosmic, precipitation, sedimentation, or built by microorganisms as in the sea plankton). Magnetic spherules, about 50 μ in diameter, collected in the Pacific red clays showed two types of structure; some of them had a metallic core (30 μ) surrounded by a layer looking like oxides; the others were mono-phased (oxides). The analysis of many particles of both types supported the theory of their cosmic origin and permitted a study of their further transformation among the deep sea sediments (65).

Scanning analysis has been used for determining the composition of fine exsolution intergrowths in natural minerals (66).

C. Technical Studies

A great help has been given to radio and TV tube builders by electron probe microanalysis of cathodes, filaments, grids, etc. The size of the analyzed region and the accuracy of the analysis are the main factors in the success of such studies of very small technical parts.

REFERENCES

1. Castaing, R., and Guinier, A., *Proc. 1st Intern. Conf. on Electron Microscopy, Delft, 1949*, pp. 60–63 (1950); Castaing, R., and Guinier, A., *Congr. intern. de Microscopie Electronique, Paris, 1950* p. 391 (1952).
2. Castaing, R., Thesis, University of Paris (1951), publ. O.N.E.R.A. No. 55.
3. Castaing, R., *Recherche aeronauti.* **23**, 41 (1951); *Natl. Bur. Standards (U. S.) Circ.* **527**, 305–309 (1954); Castaing, R., and Guinier, A., *Anal. Chem.* **25**, 724 (1953).
4. Moseley, H., *Phil. Mag.* [4] **26**, 1024 (1913); **27**, 703 (1914).
5. Dauvillier, A., *Compt. rend. Acad. Sci.* **174**, 1347 (1922); Urbain, G., *ibid.* p. 1349.
6. Coster, D., and von Hevesy, G., *Naturwissenschaften* **11**, 133 (1923).
7. Castaing, R., and Descamps, J., *J. phys. radium* **16**, 304 (1955).
8. Williams, E. J., *Proc. Roy. Soc. (London)* **A130**, 326 (1932) (read mg/cm² instead of gm/cm²!).
9. Compton, A. H., and Allison, S. K., "X-Rays in Theory and Experiment," 2nd ed., p. 76. Van Nostrand, New York, 1935 (the numerical coefficient is false by a factor 1,000).
10. Bricks, M., and Bruck, H., *Ann. radioelectricité* [3] **14**, 339 (1948).
11. Mulvey, T., *Mem. sci. Rev. mét.* **56** (2), 163 (1959).
12. Birks, L. S., and Brooks, E. J., *Rev. Sci. Instr.* **28**, 709 (1957).
13. Marton, L., and Simpson, J. A., Electron Probe Microanalyzer Conference, Washington, D. C. (Feb. 1958), report by Birks, L. S. (U. S. Naval Research Lab.).
14. Langmuir, D. B., *Proc. I.R.E.* **25**, 977 (1937).

15. Haine, M. E., and Einstein, P. A., *Brit. J. Appl. Phys.* **3**, 40 (1952).
16. Castaing, R., and Descamps, J., *Compt. rend. Acad. Sci.* **238**, 1506 (1954).
17. Castaing, R., *Compt. rend. Acad. Sci.* **231**, 835-994 (1950).
18. Marton, L., *Natl. Bur. Standards (U. S.) Circ.* **527**, 265 (1954).
19. Wittry, D. B., Thesis, California Institute of Technology (1957).
20. Cosslett, V. E., and Haine, M. E., *Proc. Intern. Conf. on Electron Microscopy, London, 1954* p. 639 (1954).
21. Dyke, W. P., Barbour, J. P., Trolan, J. K., and Martin, E. E., *Bull. Am. Phys. Soc.* **29**, 15 (1954); Dyke, W. P., Trolan, J. K., Dolan, W. W., and Grundhauser, F. J., *J. Appl. Phys.* **25**, 106 (1954).
22. Duncumb, P., and Melford, D. A., *2nd Intern. Symposium on X-Ray Microscopy and X-Ray Microanalysis, Stockholm, 1959*. Paper 52. Elsevier, Amsterdam (to be published).
23. Archard, G. D., *2nd Intern. Symposium on X-Ray Microscopy and X-Ray Microanalysis, Stockholm, 1959* Paper 48. Elsevier, Amsterdam, 1959.
24. Liebmann, G., *Proc. Phys. Soc. (London)* **64**, 972 (1951).
25. Castaing, R., and Descamps, J., *Recherche aéronaut.* **63**, 41 (1958).
26. Lenard, P., "Quantitatives über Kathodenstrahlen aller Geschwindigkeiten." Carl Winters Universitätsbuchhandlung Heidelberg, 1918.
27. Ennos, A. E., *Brit. J. Appl. Phys.* **4**, 101 (1953); **5**, 27 (1954).
28. Cambou, F., Diplôme d'Etudes Supérieures, University of Toulouse (1955).
29. Borovsky, I. B., Collection "Metallurgical Problems" (for the 70th anniversary of Acad. I. P. Bardin). Acad. Sci. U.S.S.R., 1953; Borovsky, I. B., and Ill'in, N. P., *Doklady Akad. Nauk S.S.S.R.* **106**, (4), 655 (1956).
30. Fisher, R. M., Denver Research Symposium (1956).
31. Birks, L. S., and Brooks, E. J., Electron Probe Microanalyzer Conference, Washington, D. C. (Feb. 1958), report by Birks, L. S. (U. S. Naval Research Lab.).
32. Mulvey, T., and Campbell, A. J., *Brit. J. Appl. Phys.* **9**, 406 (1958).
33. Dolby, R. M., *Proc. Phys. Soc. (London)* **73**, 81 (1959).
34. Riggs, F. B., Electron Probe Microanalyzer Conference, Washington, D. C. (Feb. 1958), report by Birks, L. S. (U. S. Naval Research Lab.).
35. Dolby, R. M., and Cosslett, V. E., *2nd Intern. Symposium on X-Ray Microscopy and X-Ray Microanalysis, Stockholm, 1959* Paper 51. Elsevier, Amsterdam (to be published).
36. Castaing, R., *Proc. Intern. Conf. on Electron Microscopy London, 1954* Paper 68 (1954).
37. Cosslett, V. E., and Duncumb, P., *Nature* **177**, 1172 (1956); Duncumb, P., Thesis, Cambridge University (1958).
38. Wittry, D. B., *J. Appl. Phys.* **29**, 1543 (1958).
39. Williams, E. J., *Proc. Roy. Soc. (London)* **A130**, 320 (1932).
40. Terrill, H. M., *Phys. Rev.* **22**, 106 (1923).
41. Duncumb, P., *2nd Intern. Symposium on X-Ray Microscopy and X-Ray Microanalysis, Stockholm, 1959* Paper 53. Elsevier, Amsterdam (to be published).
42. Castaing, R., *Rev. mét.* **52** (9) 675 (1955); Castaing, R., *Compt. rend. coll. C.N.R.S. de Toulouse* "Les Techniques Récentes en Microscopie Electronique et Corpusculaire" p. 123 (1955).
43. Blanchard, C. H., and Fano, U., *Phys. Rev.* **82**, 767 (1951).
44. Compton, A. H., and Allison, S. K., "X-Rays in Theory and Experiment:" (a) p. 105; (b) p. 71; (c) p. 99; (d) p. 79.
45. Castaing, R., and Descamps, J., *Compt. rend. Acad. Sci.* **237**, 1220 (1953).

46. Webster, D., *Proc. Natl. Acad. Sci. U. S.* **14**, 330 (1928).
47. Descamps, J., and Philibert, J., *Proc. G.A.M.S. Meeting on Non-destructive Analytical Methods, Paris, 1957*, p. 275, (1958).
48. Weill, Mrs. A. R., *Rev. mét.* **56** (4), 371 (1959).
49. Bizouard, Mrs. H., and Philibert, J., *Rev. mét.* **56** (7), 123 (1959).
50. Pomey, G., *Mem. sci. Rev. mét.* **56** (5), 471 (1959).
51. Plateau, J., Henry, G., and Philibert, J., *Compt. rend. Acad. Sci.* **246**, 2753 (1958).
52. Philibert, J., and Bizouard, Mrs. H., *Mem. sci. Rev. mét.* **56** (2), 187 (1959).
53. Crussard, C., Kohn, A., de Beaulieu, C., and Philibert, J., *Rev. mét.* **56** (4) 395 (1959).
54. Collette, G., Crussard, C., Kohn, A., Plateau, J., Pomey, G., and Weisz, M., *Rev. mét.* **54**, 433 (1957).
55. Austin, A. E., Richard, N. A., and Schwartz, C. M., *2nd Intern. Symposium on X-Ray Microscopy and X-Ray Microanalysis, Stockholm, 1959* Paper 58. Elsevier, Amsterdam (to be published).
56. Philibert, J., and de Beaulieu, C., *Rev. mét.* **56** (2), 171 (1959).
57. Melford, D. A., and Duncumb, P., *Metallurgia* **57**, 159 (1958); Melford, D. A., *2nd, Intern. Symposium on X-Ray Microscopy and X-Ray Microanalysis, Stockholm, 1959* Paper 59. Elsevier, Amsterdam (to be published).
58. Pons, M., Discussion of Philibert-Bizouard paper (52).
59. Borovsky, I. B., *2nd Intern. Symposium on X-Ray Microscopy and X-Ray Microanalysis, Stockholm, 1959* Paper 49. Elsevier, Amsterdam, 1959.
60. Adda, Y., and Philibert, J., *Proc. 2nd U.N. Intern. Conf. on Peaceful Uses of Atomic Energy, Geneva 1958*. Vol. **6**, pp. 72-90 (1958).
61. Philibert, J., and Adda, Y., *Compt. rend. Acad. Sci.* **245**, 2507 (1957).
62. Adda, Y., Beyeler, M., and Kirianenko, A., *Compt. rend. Acad. Sci.* **250**, 115 (1960).
63. Guillemin, C. and Capitant, M., unpublished; will be presented at *21st Intern. Congr. for Geology, Copenhagen* (1960).
64. Castaing, R., Philibert, J., and Crussard, C., *J. Metals* **9**, 389 (1957); Castaing, R., Philibert, J., and Crussard, C., *Trans. A.I.M.E.* **209**, 5 (1957).
65. Castaing, R., and Fredriksson, K., *Geochim. et Cosmochim. Acta* **14**, 114 (1958).
66. Agrell, S. O., and Long, J. V. P., *2nd. Intern. Symposium on X-Ray Microscopy and X-Ray Microanalysis, Stockholm, 1959* Paper 57. Elsevier, Amsterdam (to be published).